INVESTIGATION OF ELECTRODYNAMIC STABILIZATION AND CONTROL OF LONG ORBITING TETHERS

Contract NAS8-33691

Interim Report

For the period 1 September 1979 through 28 February 1981

Principal Investigator

Dr. Giuseppe Colombo

Co-Investigators

Dr. Mario D. Grossi
Dr. Marino Dobrowolny
Mr. David A. Arnold

ACKNOWLEDGEMENT

The authors of this report are:

Mr. D.A. Arnold

and

Dr. M. Dobrowolny

TABLE OF CONTENTS

INTRODUCTION

This report covers work done on NASA Contract NAS8-33691, "Investigation of Electrodynamic Stabilization and Control of Long Orbiting Tethers." In addition to the original topic of studying how electric currents could be used to control the motion of a long wire in space, the report also includes some new techniques for controlling instabilities during retrieval and an investigation of how the tether can be used for launching satellites from the Space Shuttle. The appendices to this report present derivations and analyses of a general nature used in all of the areas studied.

1. Stabilization

1.1 Introduction to Electrodynamic Stabilization

The objective of this study is to devise an algorithm for using electric currents to control pendular oscillations of the Skyhook wire induced by various perturbing forces. The electrodynamic force is perpendicular to the wire and the earth's magnetic field. The principle limitation of this technique is that the sign of the wire current (positive or negative) and the direction of the earth's magnetic field cannot be controlled so that the method offers less flexibility than thrusters. Methods have been devised for taking best advantage of favorable geometries for electrodynamic damping of tether oscillations.

1.2 Electrodynamic Equations

A wire of length $\vec{dl}$ moving at velocity $\vec{v}$ with respect to a magnetic field $\vec{B}$ experiences an electromotive force V given by $\vec{v} \times \vec{B} \cdot |\vec{dl}|$. The current I generated by this electromotive force causes a force $\vec{F} = \vec{I} \times \vec{B}\,|\vec{dl}|$ on the wire. This force is always a drag force unless the orbit is so high that the rotational velocity of the magnetic field is greater than the orbital velocity of the wire. The maximum current that can flow is V/Z where Z is the total impedance of the circuit, including the wire resistance, the contact resistance of the electrodes with the plasma, and the effective impedance of the external circuit in the plasma. The damping algorithm assumes that the desired current is within the maximum possible current. In situations where it is not, the effectiveness of the damping would be reduced.

1.3 Transverse and Vertical Forces on the Tether

The problem of controlling tether oscillations arises from the fact that the Shuttle has direct control over the tether system only through reeling or

unreeling the wire. Apart from accompanying Coriolis forces, this method allows control of only the vertical position of the subsatellite. Coriolis forces cause the subsatellite to move in the direction of the orbital motion when the subsatellite moves closer to the earth, and to lag behind the Shuttle when the motion is to higher altitudes. There is also weak coupling between the vertical and out-of-plane movements. However, damping occurs only on deployment, and reeling in the tether causes negative damping. Other forces acting transverse to the wire are the restoring force of the gravity gradient, and atmospheric drag. One can, of course, have active control of subsatellite motion using small rockets. If the wire is an electrical conductor, and currents are allowed to flow, there will be an electrodynamic force on the wire which is perpendicular to the wire and the direction of the earth's magnetic field. The electrodynamic force has the attractive property of allowing transverse forces to be applied to the wire without the expenditure of fuel or energy.

1.4 Tether Instability Modes and Causes

Tether instabilities can result during rapid retrieval as a result of Coriolis forces and residual angular momentum of the tether system with respect to the Shuttle. During station keeping, variations in atmospheric drag can excite pendular oscillations particularly when there is resonance between the natural frequency of tether oscillation and the frequency of the drag variations. The drag variations of principle concern are the diurnal bulge caused by solar heating of the atmosphere, the equator to pole variation in density arising from earth oblateness, and the corotation of the atmosphere as the earth rotates.

In an equatorial orbit, the diurnal bulge can excite in-plane oscillations. Since the perturbing force is at orbital frequency and the natural period for

in-plane oscillations i. $\sqrt{3}$ times the orbital frequency, the tether oscillation cannot stay in phase with the driving force and beats result. In-plane oscillations can also result from orbital eccentricity since the drag on the subsatellite is larger at perigee than at apogee.

In a polar orbit, in-plane oscillations can result from the diurnal bulge which causes a perturbation at orbital frequency, and the equator to pole variation from earth oblateness which causes a perturbation at twice the orbital frequency. Beat phenomena would result since neither perturbation is at the natural frequency for in-plane oscillations.

Out-of-plane drag forces will act on a subsatellite in a polar orbit as a result of the corotation of the earth's atmosphere. The force occurs twice per orbit in an easterly direction at the equator crossings. Since the out-of-plane natural oscillation frequency is twice the orbital frequency, this case must be examined in detail because of the possibility of resonant excitation of oscillations. To do this, let us use an x-y-z coordinate system with the z axis at the Northpole, the x axis in the equatorial plane, and the y axis directed to form a right handed coordinate system as shown in Figure 1.

Let us start the Shuttle and subsatellite on the x-axis with a velocity in the z direction. Since the transverse force due to corotation of the atmosphere is in the +y direction, let us assume the subsatellite has a pendulum velocity in the +y direction in addition to the orbital velocity in the z direction. Let the angular position θ of the system along the orbit be measured north from the x axis. Table 1 lists the out-of-plane position and velocity of the subsatellite in the y direction and the magnitude of the transverse drag force for the first half orbit. At $\theta = 0$, the out-of-plane velocity $\dot{y}$ is in phase with the perturbing force F_y by design in the initial conditions. At $\theta = 180°$ $\dot{y}$ is out of phase with F_y. If the magnitude of the

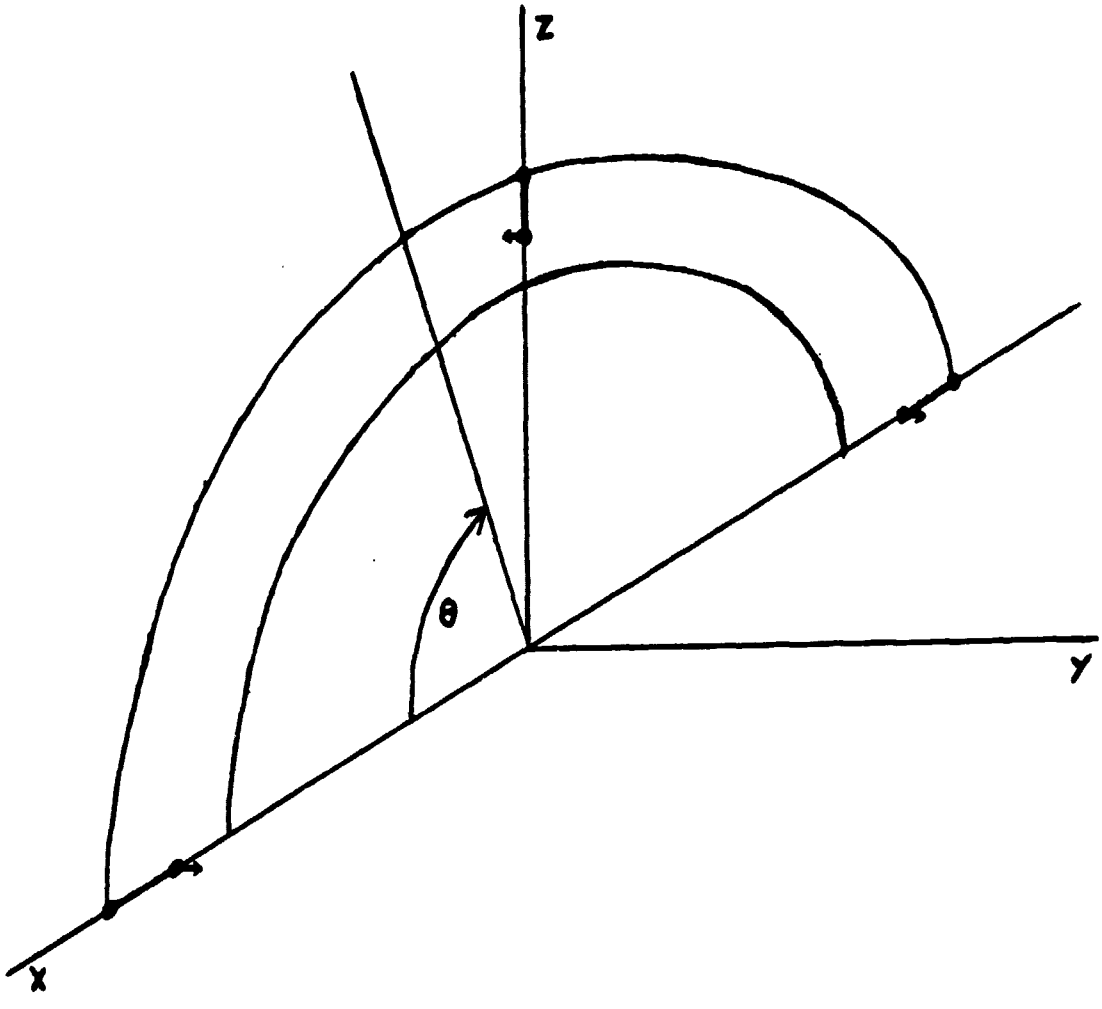

Figure 1. Coordinate system for study of out-of-plane oscillation.

Table 1. Out-of-plane position and velocity of subsatellite and perturbing force vs.-angular position along the orbit.

θ	y	$\dot{y}$	Fy
0	0	$\dot{y}_M$	F_M
45	$+y_M$	0	$F_M/\sqrt{2}$
90	0	$-\dot{y}_M$	0
135	$-y_M$	0	$-F_M/\sqrt{2}$
180	0	$+\dot{y}_M$	$-F_M$

corotation force is the same at the equator crossings on opposite sides of the earth, the perturbations oppose and tend to cancel each other. In general the forces will not be equal because of the diurnal bulge or orbital eccentricity. In this case there will be a resonant build-up of the out-of-plane oscillation.

1.5 Damping of Simple Pendulum Motion

For small oscillations the horizontal motion of a mass m at the end of a rod of length ℓ with a vertical force F_v on the mass and a damping coefficient b is

$$\ddot{mx} + \dot{bx} + \frac{F_v x}{\ell} = 0 \quad .$$

The frequency ω of the pendulum is

$$\omega = \frac{-b \pm \sqrt{b^2 - 4mF_v/\ell}}{2m}$$

To obtain critical damping, the quantity under the square root is set to zero to obtain the critical damping coefficient

$$b_C = 2\sqrt{\frac{mF_v}{\ell}}$$

The actual Skyhook system is a spherical pendulum oscillating in a rotating frame of reference. If the electrodynamic drag force were in the same plane as the pendulum oscillation one could use a damping algorithm similar to the above case for providing an electrodynamic damping force during half of the oscillation cycle. The electrodynamic force cannot be used over a full cycle unless it were possible to reverse the direction of the current. In general, the electrodynamic force will not be parallel to the velocity and the pendulum oscillation will not be confined to a plane.

1.6 Vector Damping

In Figure 2 an object with velocity $\vec{v}$ is acted on by a force $\vec{F}$. In Figure 2a, the angle θ between the velocity vector and the force vector is less than 90°. The velocity $\vec{v}$ can be resolved into components $\vec{v}_\perp$ and $\vec{v}_\parallel$ which are perpendicular and parallel respectively to the force $\vec{F}$. The force $\vec{F}$ cannot change the magnitude of $\vec{v}_\perp$. Since θ is less than 90°, $\vec{v}_\parallel$ is in the same direction as $\vec{F}$. The force $\vec{F}$ will increase the magnitude of $\vec{v}_\parallel$ and therefore increase the velocity and kinetic energy of the object. In Figure 2b, θ is greater than 90° and $\vec{v}_\parallel$ is anti-parallel to $\vec{F}$. The force $\vec{F}$ will decrease the magnitude of $\vec{v}_\parallel$ and reduce the kinetic energy of the object. The magnitude of $\vec{v}_\parallel$ can be reduced to zero at which point the angle between $\vec{v}$ and $\vec{F}$ is 90°. If $\vec{F}$ continues to act on $\vec{v}$, $\vec{v}$ will acquire a component of velocity $\vec{v}_\parallel$ which is parallel to $\vec{F}$ and the angle between $\vec{v}$ and $\vec{F}$ will be less than 90°. The situation then reverts to the case in Figure 2a. If the direction and sign of $\vec{F}$

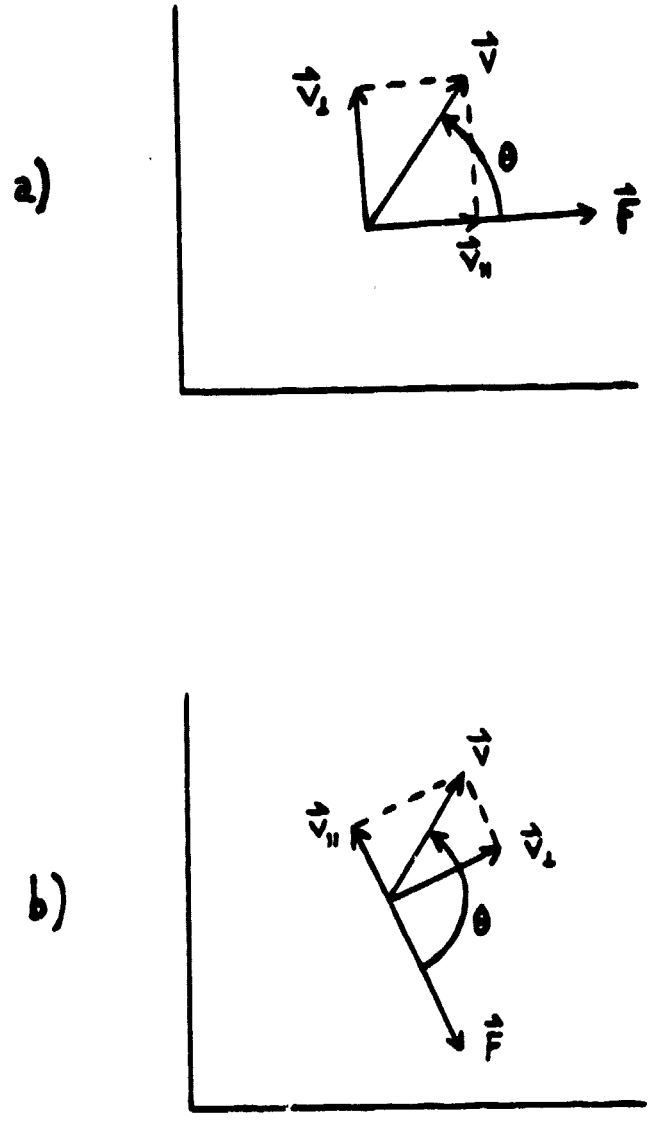

Figure 2. Force $\vec{F}$ acting on an object moving with velocity $\vec{v}$.

are fixed but the magnitude of $\vec{F}$ can be controlled, the force can be used to remove energy from the object by setting the magnitude of $\vec{F}$ proportional to the magnitude of $\vec{v}_{\parallel}$ as long as $\vec{v}_{\parallel}$ is anti-parallel to $\vec{F}$, and setting $\vec{F}$ to zero when $\vec{v}_{\parallel}$ is in the same direction as $\vec{F}$. An algorithm such as this will not add energy to the object and will remove energy whenever the geometry is favorable. The discussion above also applies in three dimensions since $\vec{v}$ can be resolved into components parallel and perpendicular to $\vec{F}$. Figure 2 can be used for three dimensional vectors by choosing axes that lie in the plane determined by $\vec{v}$ and $\vec{F}$.

1.7 Damping of Spherical Pendulum Motion

Stabilization of the Skyhook tether requires removing any velocity of the tether with respect to the equilibrium velocity of the tether. In Figure 3, $\vec{v}_2$ is the velocity of the Shuttle, $\vec{v}_1$ is the velocity of the subsatellite, and $\vec{v}_1'$ is the velocity of the equilibrium position of the tether. The vector $\vec{v}_1'$ is obtained from $\vec{v}_2$ by the equation

$$\vec{v}_1' = \vec{v}_2 \frac{r - \ell}{r}$$

where r is the distance of the Shuttle from the center of the earth and ℓ is the length of the tether. The velocity to be damped is $\Delta\vec{v}$ given by

$$\Delta\vec{v} = \vec{v}_1 - \vec{v}_1'$$

The direction of the electrodynamic force on the wire is

$$\vec{F} = \vec{I} \times \vec{B}\ell$$

The vector damping algorithm described in the previous section can be applied to the vectors $\vec{F}$ and Δv using a suitable damping coefficient b_c as described in Section 1.5. The magnitude of $\vec{F}$ can then be controlled according to the equation:

$$\vec{F} = -b_c \Delta\vec{v}_{\parallel}$$

where $\Delta\vec{v}_{\parallel}$ is the component of $\Delta\vec{v}$ parallel to $\vec{F}$.

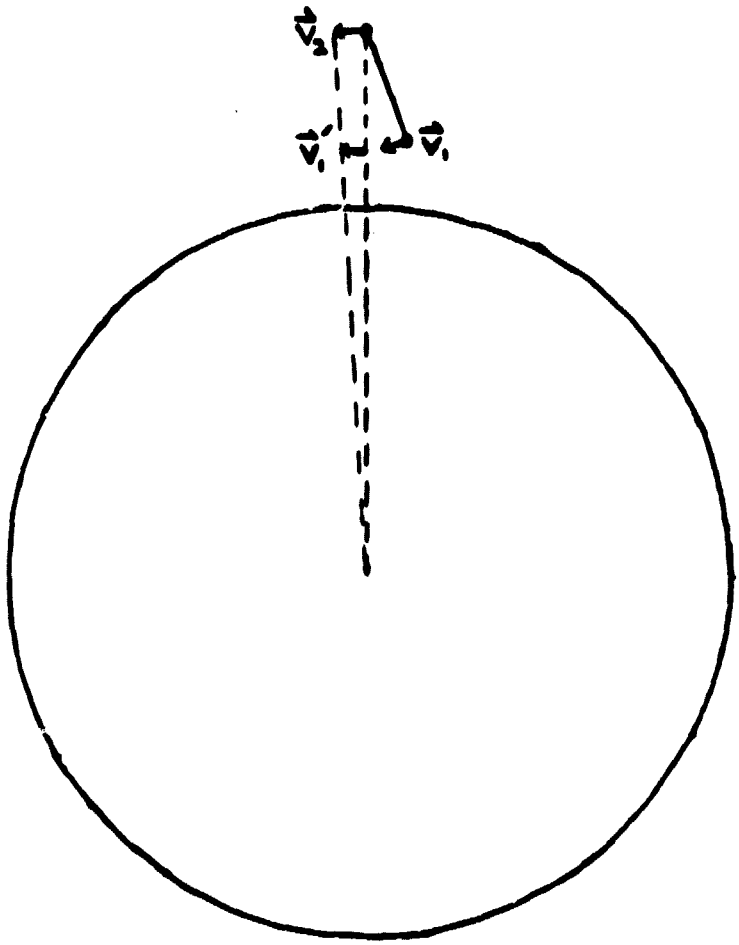

Figure 3. Velocity of the subsatellite, Shuttle, and equilibrium position of subsatellite.

In general, the electrodynamic force $\vec{F}$ and the relative velocity $\Delta\vec{v}$ will be continuously changing along the orbit of the Shuttle. The geometry will be favorable for damping at some times and not at others. The vector damping algorithm is designed to take the best advantage of opportunities for damping on a dynamic basis.

1.8 Current Generation and Control

Generation and control of currents in the Skyhook tether can be accomplished in different ways. In a completely passive mode electrons in the wire are subjected to a force arising from the tether's velocity through the magnetic field such that they are driven to the botoom of the wire (if the orbit is easterly). Assuming the wire is coated, and there are terminating electrodes, the electrostatic potential developed at the ends of the wire attracts charged particles from the plasma setting up a current loop. The current can be controlled by inserting a variable resistance between the wire and the electrode. An alternative to a collecting electrode is a plasma contactor. This would be a device that emits electrons or ions for completing the circuit to the plasma. The current could be limited by controlling the emission of electrons or ions. Such a device might be especially useful at the lower end of the wire, which collects positive ions, since collection efficiencies are low for a passive negative electrode. If the orbital geometry is such that the voltage resulting from orbital motion is small, it may be possible to drive currents with a plasma contactor that accelerates charged particles with a high voltage. This could allow electrodynamic control in cases where the electrodynamic force $\vec{F} = \vec{I} \times \vec{B}\,|\vec{\ell}|$ is non-zero, and in a useful direction, but the driving potential $\vec{v} \times \vec{B} \cdot \vec{\ell}$ is low either because $\vec{v} \times \vec{B}$ is small or the component along $\vec{\ell}$ is small. As an example, consider the case shown in Figure 1. If we neglect the offset of the magnetic pole, the magnetic field is parallel to $\vec{v}$ and therefore

there is no natural driving potential. However if a current could be forced in the wire, the electrodynamic force $\vec{F} = \vec{I} \times \vec{B}\ |\vec{\ell}|$ would be non-zero and parallel to the y axis.

The maximum current that can be obtained depends on many factors, particularly in a passive mode. The collection efficiency of electrodes depends on the size and potential of the electrodes and the ion density in the plasma. Collection of electrons is much more efficient than positive ion collection because of the high thermal velocity of electrons. The resistive limit to the current is the potential difference across the wire divided by its resistance. The potential difference from orbital motion depends on the direction of the magnetic field with respect to the orbital veloctiy.

There are various engineering considerations such as the insulation required to withstand the voltages developed in the wire, and methods of protecting payloads sensitive to high voltage. Coating the wire is necessary for accurate control of electrodynamic forces since an uncoated wire would allow uncontrolled charge collection along the wires.

1.9 Computer Program for Heuristic Study

A computer program has been written for numerical integration of the in-plane (θ) and out-of-plane (ϕ) displacements of the tether vs. time. The vector damping algorithm is included in the program.

The program is designed to run in three modes. In the first mode, there is no electrodynamic force and the tether oscillation results only from atmospheric drag. In the second mode, the current in the wire is computed as the induced voltage V divided by the tether resistance R. In the third mode, the current I is determined by the damping algorithm. This last mode assumes that the required current can be obtained and is designed to study what can be done in principle with the electrodynamic force.

When the product $\vec{I} \times \vec{B}$ becomes very small as a result of the magnetic field $\vec{B}$ being nearly parallel to $\vec{I}$, the damping algorithm calls for unreasonably large currents to compensate. To avoid this, a maximum current parameter was added to the program. The damping is still effective with the current limited to a reasonable value since the problem occurs only at certain points in the orbit. A feature is included in the program to allow the damping algorithm to operate on the vector

$$\vec{v}' = f_\theta \vec{v}_\theta + f_\phi \vec{v}_\phi$$

where f_θ and f_ϕ are weighting factors for the velocity components v_θ and v_ϕ in the θ and ϕ directions.

If the damping algorithm is applied to the out-of-plane component $\vec{v}_\phi$ of the pendulum velocity of the tether, the total velocity $\vec{v}_T$ may be either increased or decreased depending on whether the cosine of the angle α_T between the electrodynamic force $\vec{F}$ and the velocity $\vec{v}_T$, given by

$$\cos \alpha_T = \frac{\vec{F} \cdot \vec{v}_T}{|\vec{F}||\vec{v}_T|}$$

is positive or negative. The damping force is proportional to the cosine of the angle between $\vec{F}$ and $\vec{v}_\phi$ given by

$$\cos \alpha_\phi = \frac{\vec{F} \cdot \vec{v}_\phi}{|\vec{F}||\vec{v}_\phi|} \quad .$$

Some runs were done setting $|\vec{F}| = 0$. when $\cos \alpha_T > 0$. This reduces the opportunities for the damping force to be applied but guarantees that $\vec{v}_T$ will not be increased. In certain situations this condition on $\cos \alpha_T$ causes an oscillation to be set up which forces the numerical integrator to take extremely small steps, in effect halting the integration. The application of the damping force causes $\cos \alpha_T$ to become more positive. If $\cos \alpha_T$ is passing from a positive value through zero because of changes in the direction of the magnetic

field $\vec{B}$, and a damping force is suddenly applied when $\cos \alpha_T \leq 0.$, a feedback loop is created which causes the damping force to be turned on and off rapidly. The phenomenon is analogous to the cycling of a thermostat. The problem can be corrected either by having a proportional controller, or by introducing a time lag in the feedback loop to prevent rapid oscillation. The basic damping algorithm is a proportional controller since the damping force is proportional to the cosine of the angle between $\vec{F}$ and the velocity being damped. A time lag has been introduced by setting $|\vec{F}| = 0.$ for $\cos \alpha_T \geq C_{OFF}$ and setting $|\vec{F}| \sim \cos \alpha_\phi$ for $\cos \alpha_T \leq C_{ON}$. By choosing values such as $C_{ON} = -.1$ and $C_{OFF} = +.1$, rapid cycling of the damping is prevented.

Another problem causing very small integration steps occurs in near polar orbits. The induced voltage in the tether is very low and can pass through zero slowly as the orbital geometry changes. The damping algorithm was written to apply a current which ignores the value of the voltage but turns on or off as the sign of the voltage changes. The integrator takes very small steps as it approaches a change in sign of the voltage. Setting separate voltage cutoff values V_{ON} and V_{OFF} for turning the damping on and off solves the problem. The difficulty appears to be one of integrator accuracy in a grazing incidence approach to a discontinuity. No feedback oscillation was observed.

1.10 Atmospheric Model

The atmospheric density ρ is given by the equation

$$\rho = \rho_0 + \frac{\rho_E}{2}(1 + \cos 2\lambda) + \rho_D \frac{\hat{p} \cdot \hat{p}_s}{|\hat{p} \cdot \hat{p}_s|} \quad ,$$

where ρ_0 is the constant part, ρ_E is the equatorial bulge factor, λ is the latitude, ρ_D is the diurnal bulge factor, $\hat{p}$ is a unit vector pointing from the center of the earth to the Shuttle, and $\hat{p}_s$ is a unit vector pointing to the diurnal bulge. The positions of the diurnal bulge and magnetic pole, and the constants ρ_0, ρ_E, and ρ_D are input parameters to the program.

1.11 Magnetic Field Model

In the case of the earth, we can write the magnetic field $\vec{B}$ to a fairly good approximation in terms of a dipole field centered in the earth's center. In reality, the dipole is displaced from the center (by 300 km). Therefore, we can assume that

$$\vec{B} = \frac{3M_x}{r^5} x(y\hat{j} + z\hat{k}) + \frac{M_x}{r^5}(3x^2 - r^2)\hat{i}$$
$$+ \frac{3M_y}{r^5} y(z\hat{k} + x\hat{i}) + \frac{M_y}{r^5}(3y^2 - r^2)\hat{j}$$
$$+ \frac{3M_z}{r^5} z(x\hat{i} + y\hat{j}) + \frac{M_z}{r^5}(3z^2 - r^2)\hat{k} \quad ,$$

where

$$r^2 = x^2 + y^2 + z^2$$

$$x = a \cos \alpha$$

$$y = a \sin \alpha \cos i$$

$$z = a \sin \alpha \sin i$$

a = semi-major axis of the orbit

Also, with reference to Figure 4,

$$M_x = M \sin 11^\circ \cos \lambda$$

$$M_y = M \sin 11^\circ \sin \lambda$$

$$M_z = M \cos 11^\circ \cong 0.98M$$

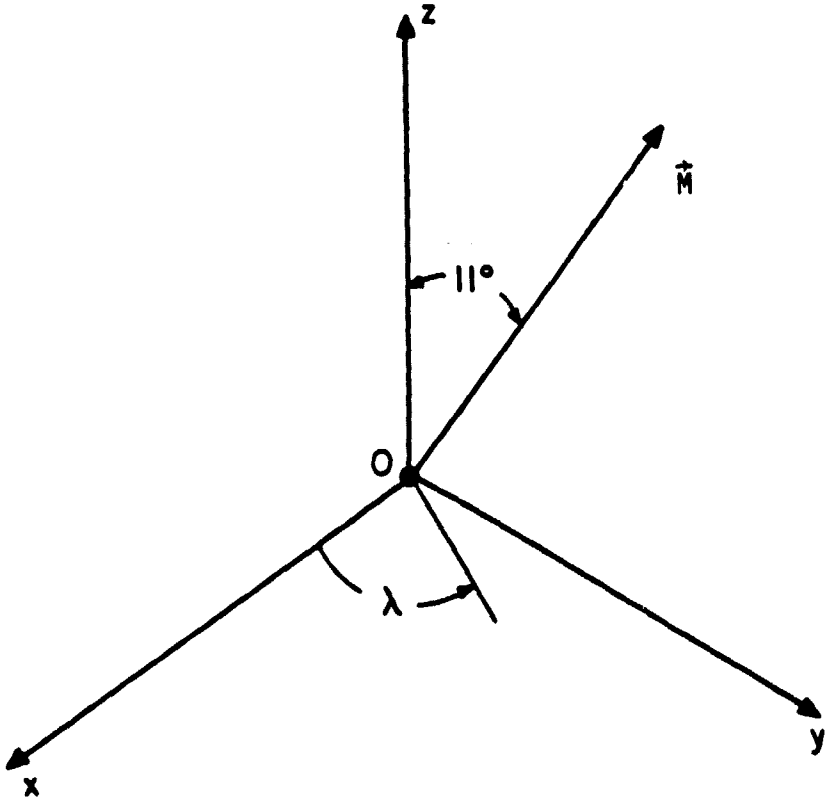

Figure 4. Reference system for the earth's magnetic field.

1.12 Cases Run in Heuristic Study

Runs have been made for equatorial, inclined, and polar or near polar orbits. In an equatorial orbit, neglecting the offset of the magnetic pole, the tether oscillation and the electrodynamic force $\vec{F}$ are both in-plane. With no damping, the in-plane oscillation due to drag perturbations show beat phenomena and there is no build-up of the amplitude with time since there is no resonance. When the damping algorithm is activated, a current is applied on the forward swing of the tether. This reduces the amplitude of the oscillations and keeps the tether closer to the equilibrium position determined by the average value of the drag force. Oscillations cannot be completely eliminated since there is always a perturbing force present.

In an inclined orbit, the drag force and electrodynamic force both have in-plane and out-of-plane components. Without damping, the in-plane oscillation shows beats as expected. The out-of-plane component is initially much smaller than the in-plane component but grows with time because the drag perturbations are resonant with the half orbital period of the out-of-plane oscillations. If the damping algorithm is applied immediately to the total velocity $\vec{v}$ of the subsatellite, the in-plane oscillation is reduced but the out-of-plane oscillation is made larger than it would be initially without damping. If the out-of-plane component is given an amplitude comparable to the in-plane oscillation, both the in-plane and out-of-plane oscillations are reduced by applying damping. If there is no initial oscillation amplitude and the damping algorithm is applied only to the out-of-plane component $\vec{v}_\phi$, the out-of-plane oscillation is prevented from building up with time and the damping currents are small, since the driving force in the out-of-plane direction is small. If the out-of-plane amplitude is initially large, and damping is applied only to $\vec{v}_\phi$, the out-of-plane oscillation is reduced to a small value, but the in-plane amplitude may be made larger than it would be without damping. This can be prevented by

applying damping to $\vec{v}_\phi$ only when the angle between $\vec{F}$ and the total velocity $\vec{v}$ is greater than 90°. Since this reduces the opportunities for damping by about a factor of two, the damping takes about twice as long and the final amplitude obtained for the out-of-plane oscillation is about a factor of two larger than that obtained with full time damping.

In a polar orbit, the electrodynamic force is in the out-of-plane direction if the offset of the magnetic pole is neglected. The induced voltage in the wire is small and exists only as result of the rotation of the magnetic field with the earth. The vectors $\vec{I}$ and $\vec{B}$ are perpendicular at the equator and parallel at the poles. If a current can be made to flow in the wire either using the naturally induced voltage in a very low resistance wire, or by using voltage sources, the electrodynamic force can be used to control the out-of-plane oscillation. This is significant since it is the out-of-plane oscillation that is subject to resonance phenomena.

Monthly Reports 3 and 4 dated December 1979 and January 1980 give the details of the runs described above. Figure 5 shows a sample plot from Monthly Report No. 4. The Shuttle is in a 220 km altitude orbit inclined 45° with respect to the equator. The tether is 10 km long and deployed upward. The out-of-plane angular velocity is initially 1.5×10^{-4} radians/sec. and the damping algorithm is applied to the out-of-plane component. Atmospheric drag is not included. Part (a) of the figure shows the in-plane angle, part (b) the out-of-plane angle, and part (c) the current. The first column in each graph is the time in seconds. The orbital period is 5333 seconds. The second column is the angle (in radians) or current (amps). The out-of-plane oscillation is quickly damped out by the damping algorithm.

In all cases described above, the damping algorithm assumes that the desired currents can be obtained by some means. The next section discusses practical considerations in generating tether currents.

FIGURE CAPTIONS

Figure 5(a). In-plane angle (radians) vs. time (sec.).

Figure 5(b). Out-of-plane angle (radians) vs time (sec.).

Figure 5(c). Damping current (amps) vs. time (sec.).

0.000	0.693483E-19
200.000	-0.272546E-02
400.000	-0.103353E-01
600.000	-0.212389E-01
800.000	-0.334494E-01
1000.000	-0.473111E-01
1200.000	-0.618965E-01
1400.000	-0.721329E-01
1600.000	-0.728383E-01
1800.000	-0.632083E-01
2000.000	-0.445506E-01
2200.000	-0.201716E-01
2400.000	0.279874E-02
2600.000	0.178440E-01
2800.000	0.219826E-01
3000.000	0.154589E-01
3200.000	0.900753E-03
3400.000	-0.176490E-01
3600.000	-0.357232E-01
3800.000	-0.495339E-01
4000.000	-0.569562E-01
4200.000	-0.573948E-01
4400.000	-0.521873E-01
4600.000	-0.433286E-01
4800.000	-0.325306E-01
5000.000	-0.213940E-01
5200.000	-0.118673E-01
5400.000	-0.578907E-02
5600.000	-0.419702E-02
5800.000	-0.715902E-02
6000.000	-0.137809E-01
6200.000	-0.224146E-01
6400.000	-0.310532E-01
6600.000	-0.378489E-01
6800.000	-0.409684E-01
7000.000	-0.392466E-01
7200.000	-0.326011E-01
7400.000	-0.218905E-01
7600.000	-0.874944E-02
7800.000	0.453067E-02
8000.000	0.153776E-01
8200.000	0.218318E-01
8400.000	0.228532E-01
8600.000	0.183954E-01
8800.000	0.932324E-02
9000.000	-0.280541E-02
9200.000	-0.160476E-01
9400.000	-0.285761E-01
9600.000	-0.388090E-01
9800.000	-0.458177E-01
10000.000	-0.492007E-01
10200.000	-0.490331E-01
10400.000	-0.458208E-01
10600.000	-0.404088E-01
10800.000	-0.330187E-01
11000.000	-0.270732E-01

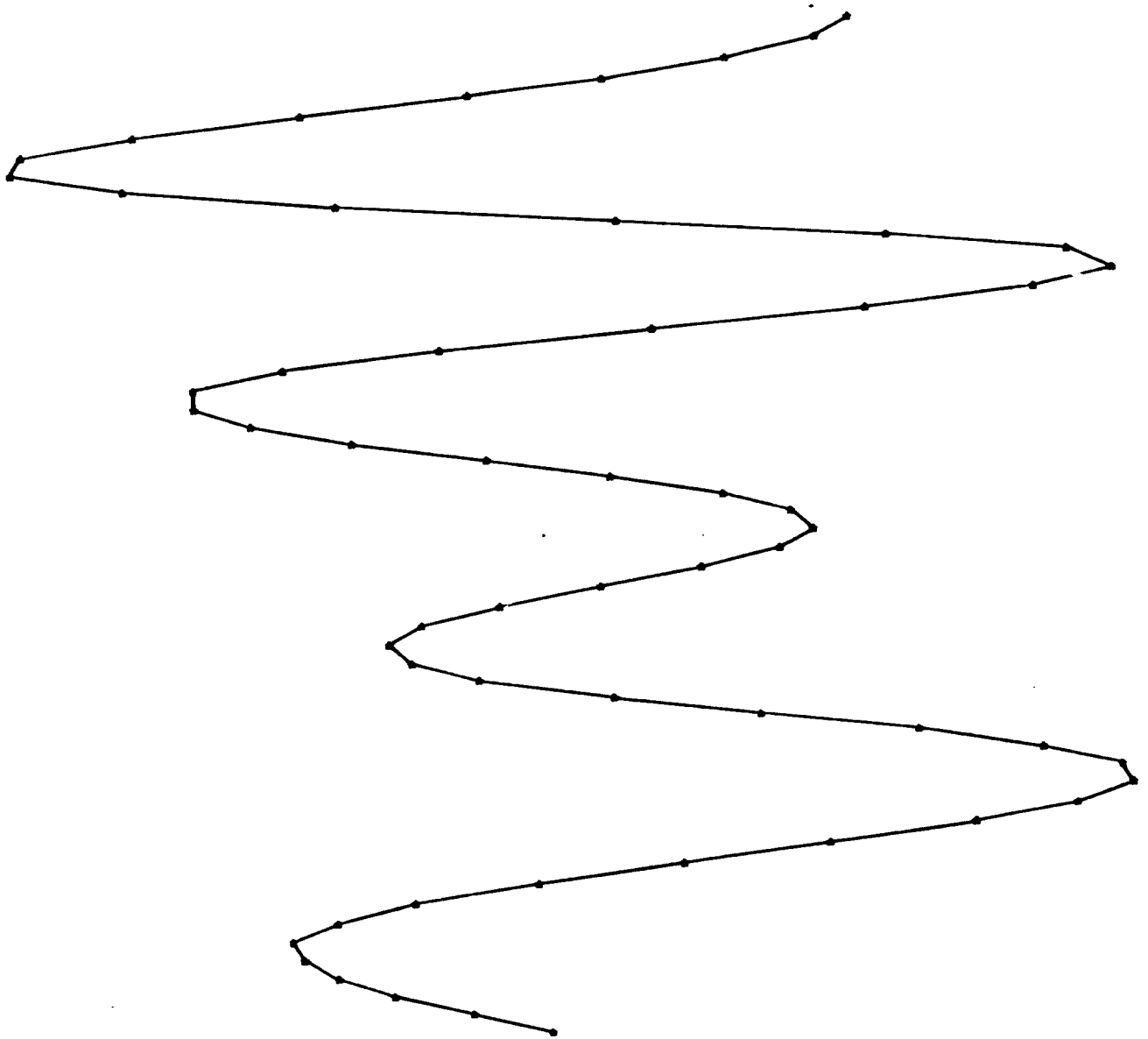

Figure 5a.

0.000	0.316534E-20
200.000	0.287788E-01
400.000	0.510506E-01
600.000	0.619940E-01
800.000	0.594799E-01
1000.000	0.456987E-01
1200.000	0.239124E-01
1400.000	-0.244777E-02
1600.000	-0.282461E-01
1800.000	-0.478659E-01
2000.000	-0.570213E-01
2200.000	-0.540307E-01
2400.000	-0.423434E-01
2600.000	-0.273981E-01
2800.000	-0.132279E-01
3000.000	-0.196392E-02
3200.000	0.572731E-02
3400.000	0.100054E-01
3600.000	0.113341E-01
3800.000	0.101249E-01
4000.000	0.672667E-02
4200.000	0.188213E-02
4400.000	-0.313311E-02
4600.000	-0.685460E-02
4800.000	-0.850294E-02
5000.000	-0.822275E-02
5200.000	-0.636061E-02
5400.000	-0.335323E-02
5600.000	0.139849E-03
5800.000	0.337680E-02
6000.000	0.569075E-02
6200.000	0.662682E-02
6400.000	0.605513E-02
6600.000	0.420325E-02
6800.000	0.145020E-02
7000.000	-0.160628E-02
7200.000	-0.428685E-02
7400.000	-0.599910E-02
7600.000	-0.636542E-02
7800.000	-0.547247E-02
8000.000	-0.391285E-02
8200.000	-0.221686E-02
8400.000	-0.714416E-03
8600.000	0.441421E-03
8800.000	0.121121E-02
9000.000	0.160667E-02
9200.000	0.164485E-02
9400.000	0.133603E-02
9600.000	0.734253E-03
9800.000	-0.984851E-05
10000.000	-0.695530E-03
10200.000	-0.118909E-02
10400.000	-0.146318E-02
10600.000	-0.156559E-02
10800.000	-0.155144E-02
11000.000	-0.143999E-02

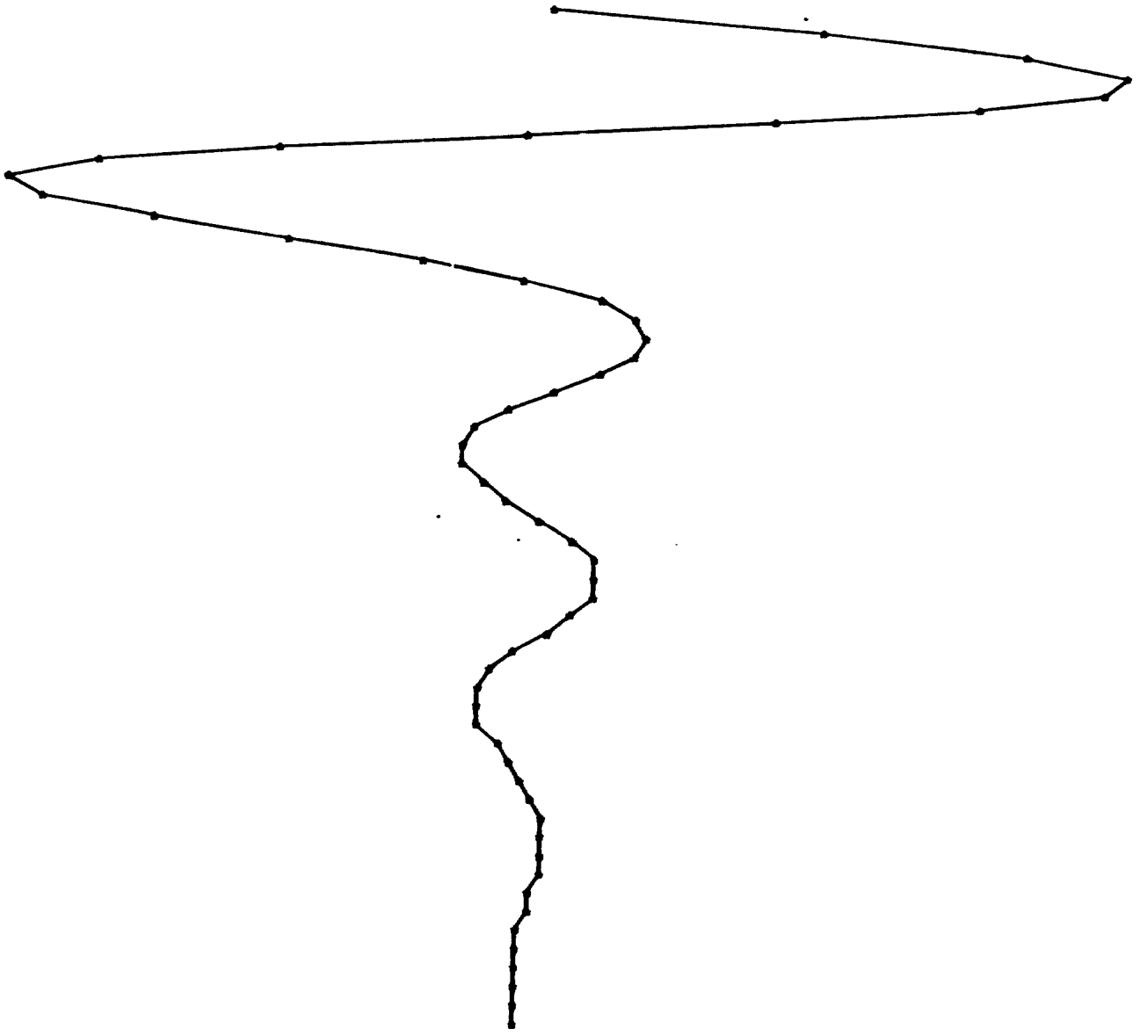

Figure 5b.

0.000	0.000000E+00
200.000	0.000000E+00
400.000	0.000000E+00
600.000	0.000000E+00
800.000	-0.931840E+00
1000.000	-0.144886E+01
1200.000	-0.874855E+00
1400.000	0.000000E+00
1600.000	0.000000E+00
1800.000	0.000000E+00
2000.000	0.000000E+00
2200.000	-0.998804E+00
2400.000	-0.167841E+01
2600.000	-0.178813E+01
2800.000	-0.152684E+01
3000.000	-0.112300E+01
3200.000	-0.600189E+00
3400.000	-0.283400E+00
3600.000	-0.156572E-03
3800.000	0.000000E+00
4000.000	0.000000E+00
4200.000	-0.272962E+00
4400.000	-0.409123E+00
4600.000	-0.295374E+00
4800.000	-0.666756E-01
5000.000	0.000000E+00
5200.000	0.000000E+00
5400.000	0.000000E+00
5600.000	0.000000E+00
5800.000	0.000000E+00
6000.000	0.000000E+00
6200.000	0.000000E+00
6400.000	-0.859502E-01
6600.000	-0.434572E-01
6800.000	0.000000E+00
7000.000	0.000000E+00
7200.000	0.000000E+00
7400.000	0.000000E+00
7600.000	-0.452002E-01
7800.000	-0.159955E+00
8000.000	-0.202217E+00
8200.000	-0.194240E+00
8400.000	-0.155732E+00
8600.000	-0.106812E+00
8800.000	-0.599481E-01
9000.000	-0.158952E-01
9200.000	0.000000E+00
9400.000	-0.910688E-02
9600.000	-0.486249E-01
9800.000	-0.729859E-01
10000.000	-0.666455E-01
10200.000	-0.443518E-01
10400.000	-0.205451E-01
10600.000	-0.488584E-02
10800.000	0.000000E+00
11000.000	0.000000E+00

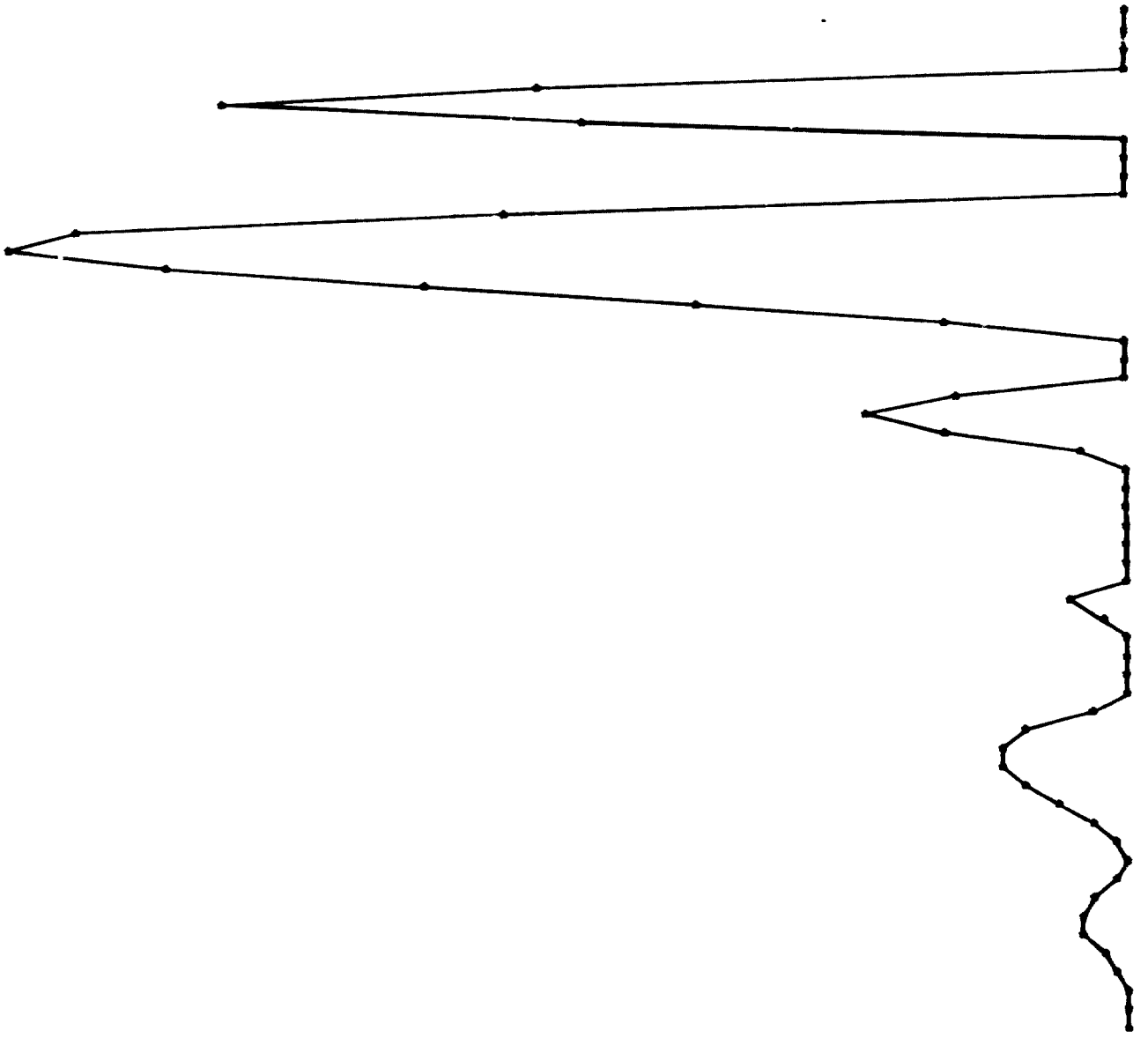

Figure 5c.

1.13 Limits to the Tether Current

In assessing plausible values for the tether current we must take into account, a) the collection of the end electrodes of the tether (conducting surface of the Shuttle at the one end and conducting balloon or subsatellite at the other end); b) the internal resistance of the tether; c) the impedance of the "circuit" external to the tether.

a) Collection of the end electrodes of the tether

An analysis of current and potentials in a coated tether configuration is contained in Reference 1 (p. 30). The numbers quoted there have taken into account only the collection properties of the electrodes. All other resistences were supposed negligible. Furthermore, a maximum electromotive force $\Delta V = VBL$ was supposed to be available ($\Delta V \sim 20$ kv for $L = 100$ km).

Table 1, Reference 1, contains a summary of limiting cases. Here by configurations A and B, we mean the cases with the Shuttle upward or downward respectively. S stands for Shuttle, b for balloon, the currents i_{j0} ($j = i, e$ for ions and electrons respectively) are thermal currents defined by

$$i_{e0} = \frac{1}{8} n_e |e| v_{the} A \qquad (1)$$

$$i_{i0} = \frac{1}{4} n_i Z |e| V_0 A \ , \qquad (2)$$

where A is the collecting area. These are essentially the currents collected by an electrode (of appropriate polarity) when its potential with respect to the plasma is small in comparison with particle thermal energies, i.e., $\frac{e\phi}{KT} \leq 1$ [in the opposite case ($e\phi/KT \gg 1$), the collection efficiency can increase very much].

Finally, for the numbers reported in Table 1, the conducting part of the Shuttle has been chosen as equivalent to a radius $r_s = 2.78$ m. Looking for example at configuration A, $L = 10^5$m and with all the available potential on the balloon (or subsatellite) we see that the current

$$i = 0.19 \text{ amps} \qquad (3)$$

corresponds to the thermal current of the Shuttle.

Increasing the balloon radius does not serve to increase the current unless very large radii are reached; where all the available potential has been displaced to the Shuttle, a situation which one clearly wants to avoid.

Notice that the same current value is also obtained (always in configuration A) for the tether of $L = 10^5$km. The only way to increase current, with respect to the value (3) would be that of using an ion gun at the Shuttle end, either increase accordingly the balloon dimensions or (in the case of a subsatellite), put an electron gun on the subsatellite.

Let us evaluate the current for a situation where, because of the orbit inclination, the driving e.m. force is very much decreased. In this limit both electrodes can be at very low potentials, so that they are only able to

draw their thermal currents. In this case we see that, for reasonable balloon or subsatellite dimensions (1.2 m radius in Table 1), the current is determined by the lower electrode and it is much smaller:

$$i \sim i_{10}(b) \sim 2.1 \times 10^{-3} \text{ amps} \quad . \tag{4}$$

Unreasonable balloon dimension would be needed to draw a current comparable to the Shuttle thermal currents. (This is because the oxygen ions are collected, at the lower electrode, at the Shuttle velocity v, whereas the electrons are collected, at the Shuttle, at their thermal velocity which is much higher).

An electron gun at the lower electrode, would allow reaching the current value of 0.19 amps determined by the Shuttle. To have more than that, again, an ion gun at the Shuttle would be necessary.

Similar considerations apply to configuration B (i.e., with the Shuttle below). In this case, referring to L = 100 km and always the Shuttle at h = 220 km, we find that

$$\frac{i_{e0(b)}}{i_{i0(s)}} \sim 1$$

for balloon radius of

$$r_b \sim 1 \text{ cm} ,$$

(as, this time, it is the balloon that collects electrons). Thus, for reasonable balloon (or subsatellite) dimensions ($r_b \sim 1$ m, for example), in a passive system and with an orbit inclination reducing drastically the e.m. force, the current in the tether is determined by the Shuttle collection and, hence, it is given by

$$i \sim 1.657 \times 10^{-2} \text{ amps} \quad . \tag{5}$$

Notice that this same current, as written in Table 1, is also obtained with all the available emf (2×10^4 volts) on the balloon for very small balloon dimensions.

To increase the current over the value (5) (taking advantage of the fact that for $r_b > 1$ cm, the balloon can drive higher currents then the Shuttle), one needs, for configuration B, an electron gun on the Shuttle.

b) Limitation due to internal tether resistance

An upper limit for the tether current, which we call resistive current i_R, is given by

$$i_R = \frac{\Delta V}{R} \tag{6}$$

where ΔV is the potential difference (due to $\underline{V} \times \underline{B}$) between the electrodes and R the electrical resistance of the tether. Figure 1 gives curves of i_R versus wire radius r_w, for steel and aluminum tethers, in the hypothesis of a maximum electromotive potential $\Delta V = VBL$. Then, for example, for a steel

tether of radius $z_w = 0.5$ mm, we get

$$i_R = 1.047 \text{ amps} \quad . \tag{7}$$

In comparing with the current values quoted above (valid for R = 0) we must however take into account that, for inclination of the orbit, such that ΔV becomes very small, the resistive current can also become very small. For example, (again for a steel tether of 0.5 mm radius) the resistive current goes to the value 1.5×10^{-2} amps, quoted above for a passive configuration A, for an angle θ between $\underline{V}$ and $\underline{B}$

$$\phi \sim 0.82 \quad . \tag{8}$$

Thus, for high inclination orbit, one may be prevented, even using guns as explained before from reaching current values $i \sim 0.1 - 1.0$ amps, useful for electrodynamic control. The only way out of this for cases where the $\underline{V} \times \underline{B}$ electromotive force becomes very small, is to use guns which also accelerate particles, thus acting as voltage generators. Essentially, in this case, the ΔV of equation (6) is supplied by the gun's acceleration with the result of avoiding the resistive limitations.

c) External impedance

The question of the external impedance or, more generally, the coupling of the tether with the lower ionosphere through magnetic flux tubes, has still to be considered quantatively (see Dobrowolny et al., 1979, for preliminary comments). In this context one must recall the early work by Drell et al., 1965, where the successive excitation of a series of transmission lines by the

motion of a large body in space was considered. We note only that the impedance of the "Alfven wings" in Drell et al. (1965) is much smaller than any reasonable tether resistance.

1.14 Conclusions

The study of electrodynamic stabilization has shown that electrodynamic forces can be used to damp pendular oscillations of the tether. The damping can be applied to the total oscillation, or to a component of the oscillation. The most useful approach appears to be to use electrodynamic forces to control the out-of-plane oscillation. The perturbing forces out-of-plane are small, but there is a resonant build-up of the amplitude, and tension control is only weakly effective on the out-of-plane component. Relatively small currents can control the out-of-plane oscillation. There is less need to control in-plane oscillations even though the perturbing force is larger because of the lack of resonance. When necessary, tension control can be used effectively for the in plane oscillation.

REFERENCES

1. M.D. Grossi. "Orbiting tether electrodynamic interactions" Final Report on Contract NASA-25077, Smithsonian Astrophys. Obs., April 1979.
2. M. Dobrowolny, D.A. Arnold, G. Colombo, and M.D. Grossi. "Mechanisms of electrodynamic interactions between a tethered satellite system and the ionosphere." Smithsonian Astrophys. Obs., Reports in Radio and Geoastronomy No. 6, August 1979.
3. S.D. Drell, H.M. Foley, and M.A. Ruderman, 1965. "Drag and propulsion of large satellites in the ionosphere: An Alfven propulsion engine in space." Journ. Geophys. Res. 70, pp. 3131-3145.

2. Retrieval

2.1 Introduction to Retrieval

One of the potential sources of unstable tether behavior is retrieval of the subsatellite. This operation can induce or amplify pendular oscillations of the tether. A study has been done to see how electrodynamic forces could be used to help stabilize the retrieval process. Some new control laws using the reel motor have been devised which can be used together with electrodynamic forces to damp oscillations of the tether.

2.2 Negative Damping of Out-of-Plane Oscillations

The coupling between the radial and out-of-plane variables introduces an acceleration $\ddot{\phi}_r$ given by

$$\ddot{\phi}_r = -2 \frac{\dot{r}}{r} \dot{\phi}$$

If $\dot{r}$ is positive (deployment), the coupling always gives positive damping since the acceleration and velocity are of opposite sign. If $\dot{r}$ is negative (retrieval), the damping is always negative except when $\dot{\phi}$ is zero. The so-called "yo-yo" approach reels in the tether at the ends of the swing while $\dot{\phi}$ is small and lets out line while $\dot{\phi}$ is large and ϕ is small. This is, of course, a time consuming method of retrieval. Electrodynamic forces can provide a way of damping this out-of-plane oscillation that is so awkward to deal with using just the reel motor. For the in-plane variable, the coupling term is $-2(\dot{\theta}+\dot{\gamma})\dot{r}\cos\phi$. Unless the magnitude of $\dot{\theta}$ is larger than the orbital angular velocity $\dot{\gamma}$ the acceleration is always in the same direction so that either negative or positive damping is possible using the reel motor.

2.3 Control Laws for Retrieval

In order to study electrodynamic control during retrieval, the general equations of motion given in Appendix A have been included in the small computer program used for the heuristic study of electrodynamic stabilization. The variables included are the in-plane angle (θ), the out-of-plane angle (ϕ) and the radial variable (r). The radial variable can be controlled either by a tension control law, or a rate control law. If the tension is controlled, the program integrates six quantities, θ, $\dot{\theta}$, ϕ, $\dot{\phi}$, r, and $\dot{r}$. The second derivatives of each variable are given by the equations of motion. If a rate control law is used, only five quantities are integrated. The sixth quantity $\dot{r}$ is specified by the rate control law. A rate control law does not guarantee positive tension. Runs done with the tension control law,

$$\text{TENSION} = 7W_o^2\ell + 4W_o\dot{\ell} - 4W_o^2\ell c$$

(eq. III-1 of NASA TMX-73314) show the expected behavior, namely a slow stable retrieval. The fastest possible retrieval is one where the tether is retrieved at a constant angle θ_r and the retrieval rate is controlled such that the coriolis forces exactly balance the restoring forces in the in-plane direction. The equation of motion for θ is

$$F\theta/m = r\cos\phi\ddot{\theta}+2(\dot{\theta}+\gamma)(\dot{r}\cos\phi-r\dot{\phi}\sin\phi) + 3r\gamma^2\cos\phi\cos\theta\sin\theta.$$

Setting $\ddot{\theta} = \ddot{\phi} = \dot{\phi} = \dot{\theta} = \phi = F_\theta = 0$ gives

$$2\dot{\gamma}\dot{r}_o + 3r\gamma^2 \cos\theta_r \sin\theta_r = 0$$

or

$$\dot{r}_o = -\frac{3}{2} r\dot{\gamma}\cos\theta_r \sin\theta_r. \qquad (9)$$

This is the rate control law for maintaining a constant retrieval angle θ_r in the absence of any perturbing forces. A run done with the computer program using this rate control law with an initial angle θ_r shows an exponentially

decreasing value of r with $\theta = \theta_r$ and $\phi = 0$.

A rate control law can also be used to provide damping in the in-plane direction. For small angles, the equation of motion for θ is

$$m\, r\, \ddot{\theta} + 3\, m\, r\, \dot{\gamma}^2 \theta = F_\theta$$

In order to have critical damping we would like to add a term $b\dot{\theta}$ to the equation where b is given by

$$\begin{aligned} b &= 2\sqrt{(mr)\ (3mr\dot{\gamma}^2)} \\ &= 2\sqrt{3}\, mr\dot{\gamma} \end{aligned} \tag{10}$$

The coriolis term in the full equation of motion for θ is

$$2m\ (\dot{\theta}+\dot{\gamma})\ \dot{r}\cos\phi \approx 2m\ (\dot{\theta}+\dot{\gamma})\ \dot{r}$$

for small values of ϕ. The value of $\dot{r}$ required to maintain a constant retrieval angle is given by equation (9). To this value of $\dot{r}$ can be added an increment $\Delta\dot{r}_1$ defined by the equation

$$b\ \dot{\theta} = 2m\ (\dot{\theta}+\dot{\gamma})\ \Delta\dot{r}_1$$

In this way the coriolis force can be adjusted to provide the necessary damping. The damping part of the rate control law is

$$\Delta\dot{r}_1 = \frac{b\dot{\theta}}{2m\ (\dot{\theta}+\dot{\gamma})}$$

Substituting the value of b from equation (10) gives

$$\Delta\dot{r}_1 = \frac{\sqrt{3}\ r\ \dot{\gamma}\ \dot{\theta}}{2m\ (\dot{\theta}+\dot{\gamma})} \tag{11}$$

A run has been made starting with $\theta = 0.$ and applying a rate control law

$$\dot{r} = \dot{r}_o + \Delta\dot{r}$$

The tether angle increases from $\theta = 0$ to $\theta = \theta_r$ smoothly, approaching θ_r exponentially. The retrieval remained stable to the end of the run. The above runs indicate that a rate control law can control the in-plane behavior in the absence of any out-of-plane oscillations or any perturbing forces.

The rate control law in equation (9) does not take into account drag or other forces on the tether. In an analytical computation, the control law could take into account the computed forces. In actual practice the forces may not be well known. The control law can include a "restoring" force to counteract deviations of the tether in-plane angle from the desired value θ_r. The restoring force should be the same order of magnitude as the restoring force,

$$3\, r\dot{\gamma}^2 \cos\phi \cos\theta \sin\theta,$$

in the general equation of motion for the in-plane angle θ. A factor k can be included to provide additional stiffness. A term $\Delta\dot{r}_2$ in the rate control law can be computed from the equation

$$2\,(\dot{\theta}+\dot{\gamma})\,\Delta\dot{r}_2 \cos\phi = -3\, r\,\dot{\gamma}^2 \cos\phi \cos\theta \sin\theta\, k\,(\theta-\theta_r)$$

which gives

$$\Delta\dot{r}_2 = -\frac{3}{2}\, r\,\dot{\gamma}^2 \cos\theta \sin\theta\, \frac{k(\theta-\theta_r)}{(\dot{\theta}+\dot{\gamma})} \quad .$$

Adding all the rate control terms we have a rate control law given by

$$\dot{r} = \dot{r}_o + \Delta\dot{r}_1 + \Delta\dot{r}_2 \quad .$$

In order to maintain critical damping, the damping part of the rate control is increased by the factor $\sqrt{k+1}$. The restoring force from $\Delta\dot{r}_2$ has the effect of speeding up the retrieval in the case where the subsatellite is above the Shuttle, and slowing down the retrieval for downward deployment.

2.4 Cases Run

In runs done for downward deployment, the restoring term halts the retrieval a few hundred meters from the Shuttle. For the upward deployment case, drag can be counteracted longer, but the dynamic eventually becomes unstable. For either case, alternative techniques must be used to control the subsatellite close to the Shuttle. Reasonable values of current in the wire (a fraction of an ampere) appear to be capable of controlling the out-of-plane oscillations in an inclined orbit. Special considerations apply to equatorial orbits or orbits passing near the magnetic pole.

Details of the cases described above are given in Monthly Reports 6 and 7 dated April and May 1980. Figure 6 shows a sample plot from Monthly Report No. 6. The Shuttle altitude is 220 km, the orbital inclination is 45 degrees and the tether length is 10 km deployed upward. The initial in-plane angle is .4 radians (lagging the Shuttle) and the out-of-plane angle is .035 radians. A rate control law with damping is used for the in-plane angle, and electrodynamic damping is used for the out-of-plane angle. There is no atmospheric drag. Part (a) of the plot is the in-plane angle, part (b) is the out-of-plane angle, part (c) is the radial distance, and part (d) is the damping current. The first column in each plot is the time in seconds and the second column is the variable being plotted. The behavior is reasonably stable at 12,000 seconds when the distance is about 5 meters.

2.5 Conclusions

It appears that electrodynamic damping can be useful for controlling the out-of-plane oscillations during retrieval. The in-plane angle can be controlled using a rate control law which includes damping and restoring terms. Differential drag between the Shuttle and the subsatellite will eventually destabilize the retrieval process when the tether length becomes too short. Other techniques must be used to control the subsatellite during the last stages of retrieval.

FIGURE CAPTIONS

Figure 6(a). In-plane angle (radians) vs. time (sec.).

Figure 6(b). Out-of-plane angle (radians) vs. time (sec.).

Figure 6(c). Radial distance (cm) vs. time (sec.).

Figure 6(d). Damping currrent (amps.) vs. time (sec.).

0.000	0.400000E+00
200.000	0.399545E+00
400.000	0.397149E+00
600.000	0.392690E+00
800.000	0.387179E+00
1000.000	0.381930E+00
1200.000	0.378056E+00
1400.000	0.376266E+00
1600.000	0.376018E+00
1800.000	0.379165E+00
2000.000	0.382331E+00
2200.000	0.384901E+00
2400.000	0.385547E+00
2600.000	0.384751E+00
2800.000	0.384185E+00
3000.000	0.385019E+00
3200.000	0.386802E+00
3400.000	0.388958E+00
3600.000	0.391171E+00
3800.000	0.393295E+00
4000.000	0.395253E+00
4200.000	0.396946E+00
4400.000	0.398135E+00
4600.000	0.398015E+00
4800.000	0.397609E+00
5000.000	0.397489E+00
5200.000	0.397947E+00
5400.000	0.399216E+00
5600.000	0.401087E+00
5800.000	0.402735E+00
6000.000	0.400563E+00
6200.000	0.389417E+00
6400.000	0.369741E+00
6600.000	0.345332E+00
6800.000	0.321332E+00
7000.000	0.303676E+00
7200.000	0.298638E+00
7400.000	0.306110E+00
7600.000	0.317652E+00
7800.000	0.321888E+00
8000.000	0.315055E+00
8200.000	0.301372E+00
8400.000	0.288173E+00
8600.000	0.282036E+00
8800.000	0.286502E+00
9000.000	0.299677E+00
9200.000	0.316369E+00
9400.000	0.333482E+00
9600.000	0.349806E+00
9800.000	0.364965E+00
10000.000	0.378289E+00
10200.000	0.387717E+00
10400.000	0.393453E+00
10600.000	0.395508E+00
10800.000	0.395549E+00
11000.000	0.397164E+00
11200.000	0.404093E+00
11400.000	0.416984E+00
11600.000	0.430806E+00
11800.000	0.434014E+00
12000.000	0.406980E+00

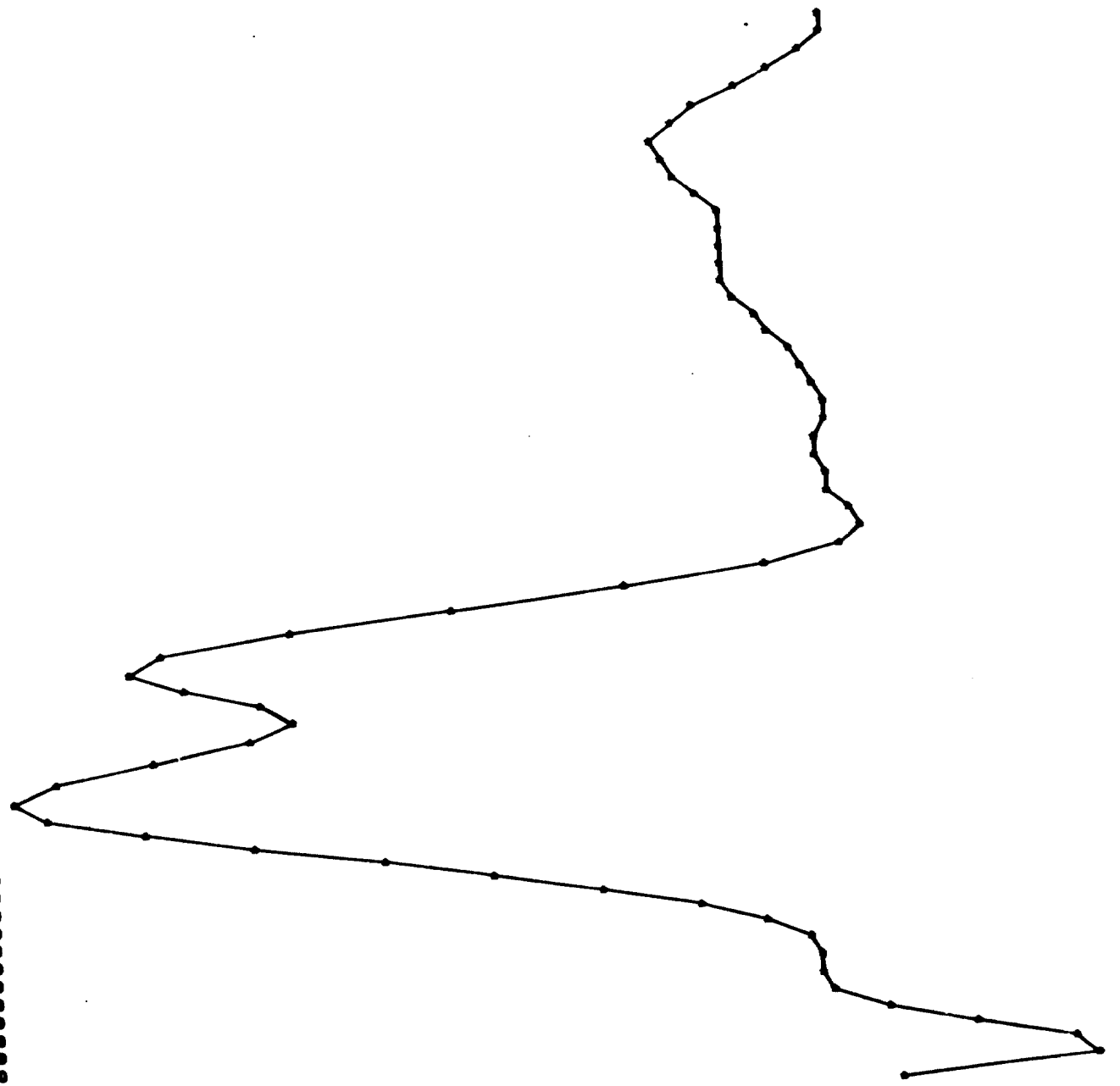

Figure 6a.

0.000	0.350000E-01
200.000	0.318526E-01
400.000	0.239731E-01
600.000	0.139457E-01
800.000	0.400078E-02
1000.000	-0.433566E-02
1200.000	-0.102489E-01
1400.000	-0.134533E-01
1600.000	-0.138912E-01
1800.000	-0.113119E-01
2000.000	-0.549759E-02
2200.000	0.292334E-02
2400.000	0.117860E-01
2600.000	0.182577E-01
2800.000	0.206279E-01
3000.000	0.186581E-01
3200.000	0.119055E-01
3400.000	0.783510E-03
3600.000	-0.137166E-01
3800.000	-0.292214E-01
4000.000	-0.425928E-01
4200.000	-0.503038E-01
4400.000	-0.491274E-01
4600.000	-0.378437E-01
4800.000	-0.133501E-01
5000.000	0.281520E-01
5200.000	0.588544E-01
5400.000	0.956249E-01
5600.000	0.121701E+00
5800.000	0.128697E+00
6000.000	0.113162E+00
6200.000	0.815693E-01
6400.000	0.406298E-01
6600.000	-0.425354E-02
6800.000	-0.487977E-01
7000.000	-0.894652E-01
7200.000	-0.121043E+00
7400.000	-0.133733E+00
7600.000	-0.119879E+00
7800.000	-0.832819E-01
8000.000	-0.352701E-01
8200.000	0.121542E-01
8400.000	0.489955E-01
8600.000	0.692400E-01
8800.000	0.721350E-01
9000.000	0.584399E-01
9200.000	0.280263E-01
9400.000	-0.155073E-01
9600.000	-0.652424E-01
9800.000	-0.111163E+00
10000.000	-0.142603E+00
10200.000	-0.149715E+00
10400.000	-0.125574E+00
10600.000	-0.672315E-01
10800.000	0.225747E-01
11000.000	0.133116E+00
11200.000	0.244638E+00
11400.000	0.331023E+00
11600.000	0.371202E+00
11800.000	0.340279E+00
12000.000	0.263945E+00

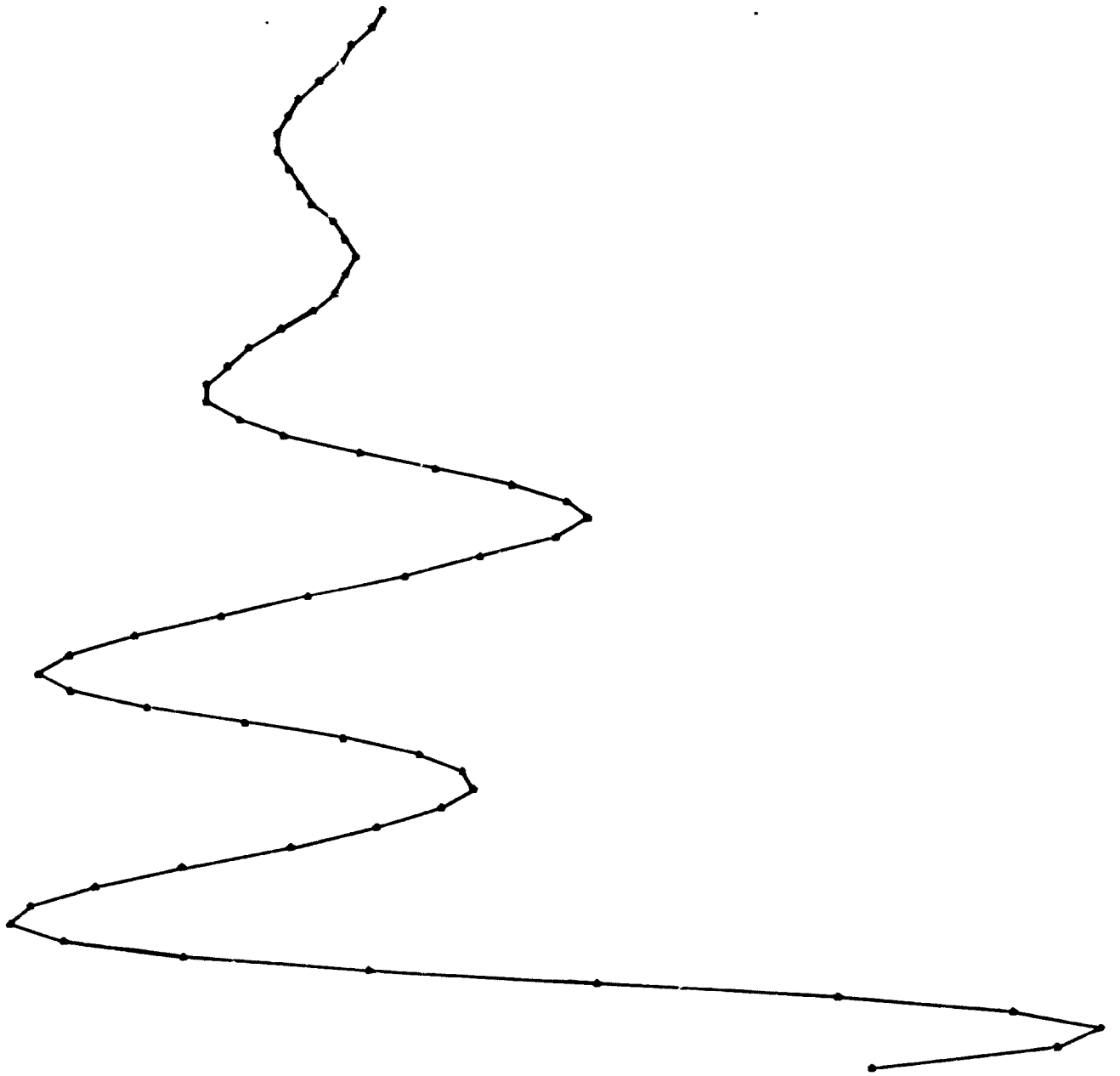

Figure 6b.

0.000	0.100000E+07
200.000	0.880250E+06
400.000	0.772206E+06
600.000	0.674937E+06
800.000	0.588801E+06
1000.000	0.513900E+06
1200.000	0.449640E+06
1400.000	0.394872E+06
1600.000	0.348187E+06
1800.000	0.307975E+06
2000.000	0.272782E+06
2200.000	0.241366E+06
2400.000	0.212867E+06
2600.000	0.187265E+06
2800.000	0.164809E+06
3000.000	0.145396E+06
3200.000	0.128480E+06
3400.000	0.113603E+06
3600.000	0.100459E+06
3800.000	0.888225E+05
4000.000	0.785115E+05
4200.000	0.693661E+05
4400.000	0.612331E+05
4600.000	0.539317E+05
4800.000	0.474776E+05
5000.000	0.418165E+05
5200.000	0.368672E+05
5400.000	0.325491E+05
5600.000	0.287664E+05
5800.000	0.254136E+05
6000.000	0.223023E+05
6200.000	0.192518E+05
6400.000	0.163401E+05
6600.000	0.137315E+05
6800.000	0.115495E+05
7000.000	0.984294E+04
7200.000	0.859286E+04
7400.000	0.766505E+04
7600.000	0.688240E+04
7800.000	0.610644E+04
8000.000	0.531392E+04
8200.000	0.456493E+04
8400.000	0.392518E+04
8600.000	0.342013E+04
8800.000	0.303570E+04
9000.000	0.273266E+04
9200.000	0.247321E+04
9400.000	0.223981E+04
9600.000	0.202602E+04
9800.000	0.182939E+04
10000.000	0.164718E+04
10200.000	0.147403E+04
10400.000	0.131118E+04
10600.000	0.115916E+04
10800.000	0.102123E+04
11000.000	0.902142E+03
11200.000	0.804040E+03
11400.000	0.723462E+03
11600.000	0.651904E+03
11800.000	0.577290E+03
12000.000	0.481812E+03

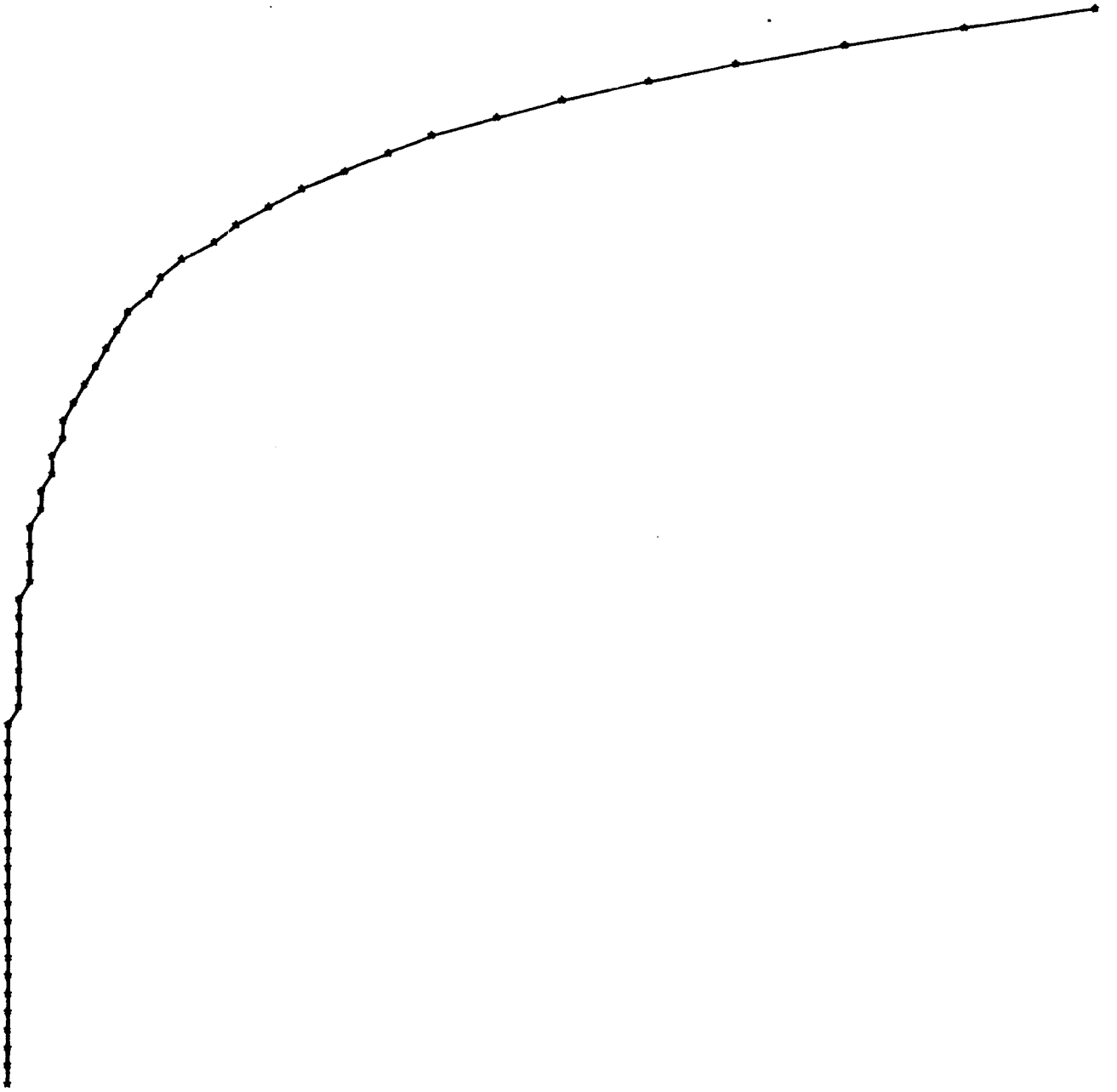

Figure 6c.

0.000	-0.413196E-08
200.000	-0.712082E+00
400.000	-0.110482E+01
600.000	-0.118601E+01
800.000	-0.108665E+01
1000.000	-0.850343E+00
1200.000	-0.505468E+00
1400.000	-0.161615E+00
1600.000	0.000000E+00
1800.000	0.000000E+00
2000.000	-0.228809E+00
2200.000	-0.765803E+00
2400.000	-0.851219E+00
2600.000	-0.487350E+00
2800.000	-0.156438E-01
3000.000	0.000000E+00
3200.000	0.000000E+00
3400.000	0.000000E+00
3600.000	0.000000E+00
3800.000	0.000000E+00
4000.000	0.000000E+00
4200.000	0.000000E+00
4400.000	-0.332114E+00
4600.000	0.000000E+00
4800.000	0.000000E+00
5000.000	0.000000E+00
5200.000	0.000000E+00
5400.000	0.000000E+00
5600.000	0.000000E+00
5800.000	-0.612082E+00
6000.000	-0.272240E+01
6200.000	-0.407560E+01
6400.000	-0.482419E+01
6600.000	-0.519442E+01
6800.000	-0.455490E+01
7000.000	-0.213443E+01
7200.000	0.000000E+00
7400.000	-0.116393E-01
7600.000	-0.339599E+01
7800.000	-0.559235E+01
8000.000	-0.592089E+01
8200.000	-0.504661E+01
8400.000	-0.337746E+01
8600.000	-0.139926E+01
8800.000	0.000000E+00
9000.000	0.000000E+00
9200.000	0.000000E+00
9400.000	0.000000E+00
9600.000	0.000000E+00
9800.000	0.000000E+00
10000.000	-0.451269E+00
10200.000	0.000000E+00
10400.000	0.000000E+00
10600.000	0.000000E+00
10800.000	0.000000E+00
11000.000	0.000000E+00
11200.000	0.000000E+00
11400.000	0.000000E+00
11600.000	0.000000E+00
11800.000	-0.394218E+01
12000.000	-0.818805E+01 *

$

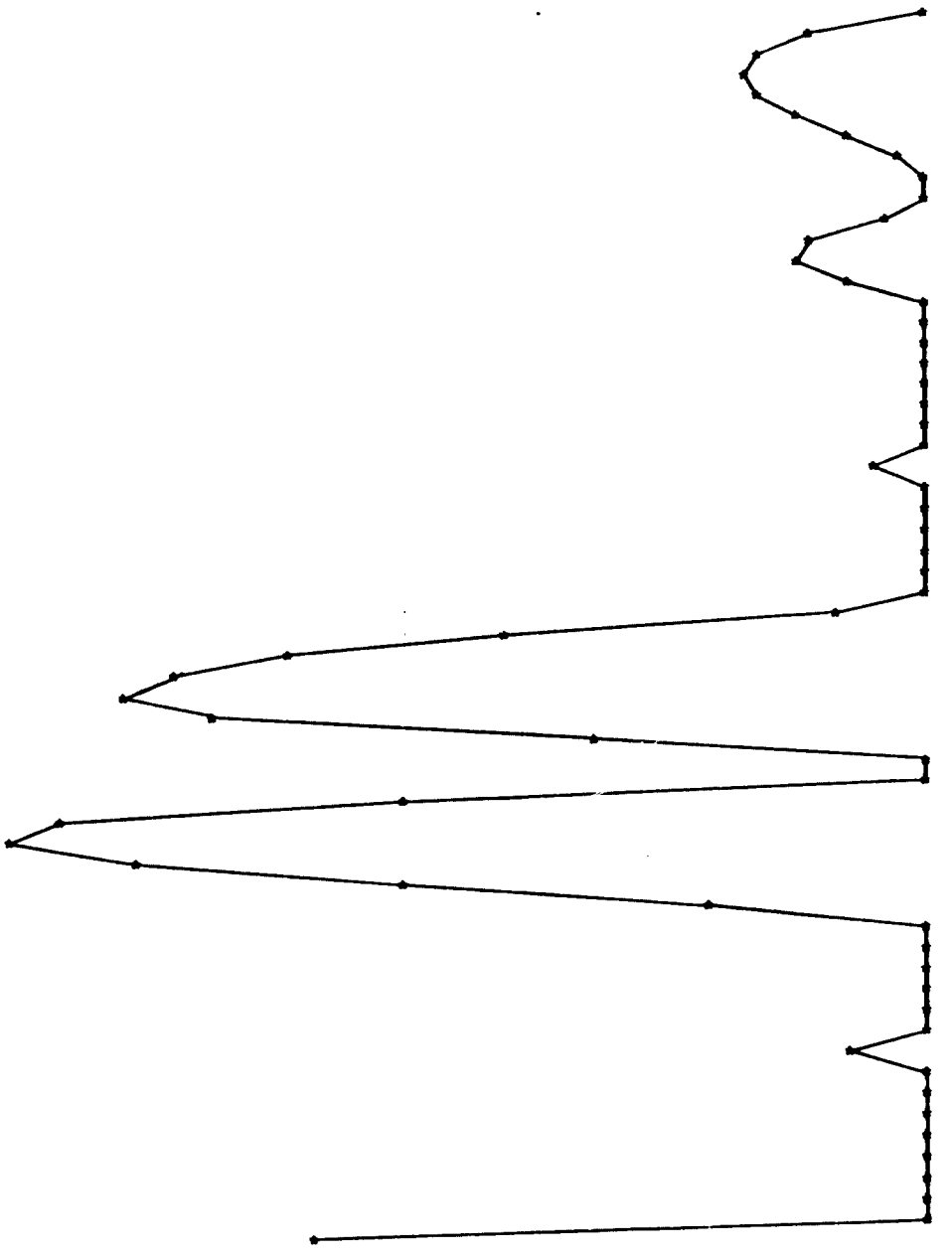

Figure 6d.

3. Launcher

3.1 Introduction to Tether Launcher

The objective of this study is to develop techniques for using the tether to launch satellites from the Shuttle. Satellites could be launched either by simply releasing them at the end of the tether or releasing them after acceleration by a rocket. The principle problem that must be studied in the dynamics of the tether itself. The techniques must be such as to avoid breakage of the tether, or loss of tension or dynamic instabilities that could lead to loss of control of the tether. Acceleration of the payload by a rocket induces various tether motions that must be carefully studied.

3.2 Subsatellite Thruster Model

The SAO Skyhook software package has been modified to include thrusters on the subsatellite. We have adopted a model with three independent thrusters in the in-plane, out-of-plane, and radial directions. The directions of the thrusters are shown in Figure 7. The Shuttle is at the origin O. The x axis is parallel to the vector from the center of the earth to the Shuttle, the z axis is normal to the orbital plane, and the y axis is perpendicular to the x-z plane in the direction of the orbital motion. The vector $\vec{r}$ goes from the

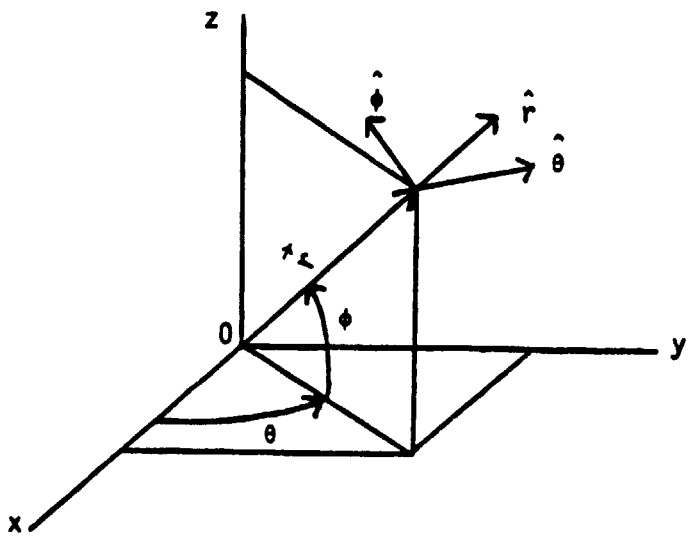

Figure 7. Coordinate system for thruster on subsatellite.

Shuttle to the subsatellite. The in-plane angle is θ and the out-of-plane angle is ϕ. The in-plane thruster is in the direction of $\hat{\theta}$, the out-of-plane thruster is in the $\hat{\phi}$ direction and the radial thruster is in the $\hat{r}$ direction.

The Skyhook software computes the directions of the in-plane, out-of-plane, and radial vectors for the Shuttle and components of the vector $\vec{r}$ along these directions. The sign convention is different from that used in Figure 7, so that the in-plane direction is in the minus y direction (opposed to the orbital velocity) and the out-of-plane direction is in the minus z direction. Ths sign convention is the same in the radial direction. The equations for the unit vectors giving the directions of the three thrusters are:

$$\hat{r} = \frac{x}{y}\hat{x} + \frac{y}{r}\hat{y} + \frac{z}{r}\hat{z}$$

$$\hat{\theta} = -\frac{y}{\rho}\hat{x} + \frac{x}{\rho}\hat{y}$$

$$\hat{\phi} = -\frac{xz}{r\rho}\hat{x} - \frac{yz}{r\rho}\hat{y} + \frac{\rho}{r}\hat{z}$$

where:

$$r = \sqrt{x^2 + y^2 + z^2}$$

$$\rho = \sqrt{x^2 + y^2}$$

The Skyhook software has been modified to read in accelerations to be applied in each of the three directions and the time period over which the accelerations are applied. Provision has been made for specifying the accelerations during two time periods so that the system can be accelerated and then decelerated.

3.3 Wire Oscillations Induced by Subsatellite Thrusters

The following two sections present analytic expressions for estimating the transverse and longitudinal wire velocities that would be induced when the subsatellite is accelerated by thrusters. For the transverse velocity a

simplified model is used where the wire mass is represented by a lump halfway between the Shuttle and subsatellite. In fact, the wire motion consists of a transverse wave travelling down the wire. The present analysis was done for the purpose of order of magnitude estimation of the dynamics of the wire. The analysis of transverse oscillations assumes the duration of the acceleration and deceleration is short compared to the natural period for transverse oscillations. Transverse motion of the subsatellite introduces coriolis effects which can increase the wire tension. In the case of short tethers especially, the coriolis effects may be many times larger than the equilibrium value of the tension.

If the wire tension is nearly constant during the acceleration and deceleration of the subsatellite, the amplitude of the transverse wire oscillation is approximately equal to the distance travelled by the subsatellite. This may be the case when the tether is long, the velocity is low, or the tether does not have enough time to stretch in response to the coriolis forces. In cases where the tension increases by a large factor during acceleration and then drops again at the end of the deceleration period, the wire may be given a large velocity which cannot be restrained by the remaining tension in the wire. If the transverse velocity acquired is larger than the velocity for a large amplitude oscillation, instability will result.

The formulas derived in the next two sections have been compared with the results of numerical integrations done with the Skyhook computer program. The details of the comparison are given in Monthly Report No. 10 dated July 1980.

3.4 Transverse Wire Velocity Induced by Subsatellite Thrusters

Approximate analytic expressions have been derived for estimating the magnitude of the transverse wire velocity that will be induced during the acceleration and deceleration of the subsatellite. In the diagram below, the

wire is represented by the mass m halfway between the Shuttle at the bottom and the maneuverable subsatellite at the top.

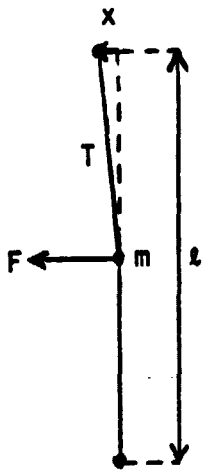

Figure 8.

The force F accelerating the wire mass is

$$F = Tx \,/\, (\ell/2) = 2\,T\,x/\ell$$

where T is the wire tension. The velocity imparted to the mass is

$$\Delta v_w = \int_{t_1}^{t_2} \frac{2Tx}{m_w \ell}\, dt \tag{12}$$

The wire tension T for an in-plane launch using equation A32 with $\ddot{r} = 0$ and $r = \ell$ is given by

$$T = 3m_s \ell \dot{\gamma}^2 + m_s \ell \dot{\theta}^2 + 2m_s \ell \dot{\theta} \dot{\gamma} \tag{13}$$

where $\dot{\gamma}$ is the orbital angular velocity, m_s is the mass of the subsatellite, $\dot{\theta}$ is v/ℓ, and v is the subsatellite velocity.

Let us assume that the subsatellite is subjected to a linear acceleration or deceleration lasting from t_1 to t_2 and that the initial velocity at t_1 is v_1. We can then derive an analytic expression for Δv_w that can be used for the acceleration, coast or deceleration period. The velocity of the subsatellite as a function of time is

$$v = v_1 + a(t-t_1) = (v_1 - at_1) + at \equiv v_1 + at \tag{14}$$

where

$$v_1 \equiv v_1 - at_1 \tag{15}$$

The angular velocity needed for equation (13) is

$$\dot{\theta} = \frac{v}{\ell} = \frac{V_1 + at}{\ell} \tag{16}$$

The position as a function of time is

$$x = x_1 + \int_{t_1}^{t} v dt = x_1 + \int_{t_1}^{t} (V_1 + at)\, dt \tag{17}$$

where x_1 is the position at time t_1. Performing the integration gives

$$x = X_o + X_1 t + X_2 t^2 \tag{18}$$

where

$$X_o \equiv x_1 - V_1 t - \frac{1}{2} a t_1^2 \tag{19a}$$

$$X_1 = V_1 \tag{19b}$$

$$X_2 = \frac{1}{2} a \tag{19c}$$

Substituting equation (16) into equation (13) gives

$$T = T_o + T_1 t + T_2 t^2 \tag{20}$$

when

$$T_o \equiv 3m_s \ell \dot{\gamma}^2 + \frac{m_s}{\ell} V_1^2 + 2 m_s V_1 \dot{\gamma} \tag{21a}$$

$$T_1 \equiv 2 \frac{m_s}{\ell} a V_1 + 2m_s a \dot{\gamma} \tag{21b}$$

$$T_2 \equiv \frac{m_s}{\ell} a^2 \tag{21c}$$

Multiplying equations (18) and (20) gives

$$Tx = C_o + C_1 t + C_2 t^2 + C_3 t^3 + C_4 t^4 \tag{22}$$

where

$$C_o = T_o X_o \tag{23a}$$

$$C_1 = T_o X_1 + T_1 X_o \tag{23b}$$

$$C_2 = T_o X_2 + T_1 X_1 + T_2 X_o \tag{23c}$$

$$C_3 = T_1 X_2 + T_2 X_1 \tag{23d}$$

$$C_4 = T_2 X_2 \tag{23e}$$

Integrating equation (22) from t_1 to t_2 gives

$$\int_{t_1}^{t_2} Tx\, dt = C_o(t_2-t_1) + \frac{C_1}{2}(t_2^2-t_1^2) + \frac{C_2}{3}(t_2^3-t_1^3) + \frac{C_3}{4}(t_2^4-t_1^4) + \frac{C_4}{5}(t_2^5-t_1^5) \tag{24}$$

Substituting (24) and (12) gives the desired expression for the velocity increment Δv_w.

In the special case where $t_1 = v_1 = x_1 = 0.$, the integration of the product Tx can be done easily. The velocity, position, and angular velocity as a function of time are

$$v = a\, t,$$

$$x = \frac{1}{2}\, a\, t^2$$

and

$$\dot{\theta} = v/\ell = at/\ell\ .$$

The tension given by equation (13) becomes

$$T = 3m_s \ell \dot{\gamma}^2 + m_s \ell \left(\frac{at}{\ell}\right)^2 + 2m_s \ell \left(\frac{at}{\ell}\right) \dot{\gamma}$$

$$= 3m_s \ell \dot{\gamma}^2 + m_s a^2 t^2 / \ell + 2m_s at\dot{\gamma}\ .$$

Multiplying by x gives,

$$Tx = \frac{3}{2} m_s a \ell \dot{\gamma}^2 t^2 + \frac{1}{2} m_s a^3 t^4/\ell + m_s a^2 t^3 \dot{\gamma} \quad .$$

Integrating with respect to time we have

$$\int_0^t Tx\,dt = \frac{1}{2} m_s a \ell \dot{\gamma}^2 t^3 + \frac{1}{10} m_s a^3 t^5/\ell + \frac{1}{4} m_s a^2 \dot{\gamma} t^4 \quad .$$

Substituting this into equation (1) gives

$$\Delta v_w = \frac{m_s}{m_w} \left(a \dot{\gamma}^2 t^3 + \frac{1}{5} a^3 t^5/\ell^2 + \frac{1}{2} a^2 \dot{\gamma} t^4/\ell \right) \tag{25}$$

Since Δv_w in equation (12) is proportional to the integral of Tx, it is desirable to minimize the amount of time the subsatellite spends at high velocity in order to reduce the excitation of transverse wire oscillations.

3.5 Radial Velocity Induced by Transverse Thrusters

Transverse velocity of the subsatellite produces a radial acceleration because of coriolis forces. From equation A32, we have for $\dot{\phi} = 0$ and $r = \ell$,

$$\ddot{r} = F_r/m + \ell \dot{\theta}^2 + 2\ell \dot{\theta} \dot{\gamma} + 3\ell \dot{\gamma}^2 \tag{26}$$

If the system is close to equilibrium the first and last terms in (26) nearly cancel each other so that

$$\ddot{r} \approx \ell \dot{\theta}^2 + 2\ell \dot{\theta} \dot{\gamma} \tag{27}$$

If the velocity is given by equation (14) we have, substituting equation (16) into equation (27),

$$\ddot{r} = R_o + R_1 t + R_2 t^2 \tag{28}$$

where

$$R_o = V_1^2/\ell + 2V_1 \dot{\gamma} \tag{29a}$$

$$R_1 = 2a(V_1/\ell + \dot{\gamma}) \tag{29b}$$

$$R_2 = a^2/\ell \tag{29c}$$

Integrating equation (28) we have

$$\Delta v_r = \int_{t_1}^{t_2} \ddot{r}\, dt$$

$$= R_o(t_2-t_1) + \frac{R_1}{2}(t_2^2-t_1^2) + \frac{R_2}{3}(t_2^3-t_1^3) \qquad (30)$$

The radial velocity Δv_r can be minimized by having the subsatellite spend as little time as possible at high velocity.

The analysis in this section can be applied to an out-of-plane launch by using the equation

$$T = 3m_s \ell \dot{\gamma}^2 + m_s \ell \dot{\phi}^2$$

instead of equation (13). Note that there is no cross term $\dot{\phi}\dot{\gamma}$ in an out-of-plane launch.

3.6 Tension Variations Caused by Transverse Wire Oscillations

The acceleration of the subsatellite by thruster induces transverse wire oscillations. These wire oscillations cause tension variations at the natural frequency for transverse oscillations by causing an acceleration $\ddot{r}$ in the radial direction. The corresponding tension variation is $m\ddot{r}$ where m is the mass of the subsatellite. In Figure 9 below, the wire mass is represented by a lumped mass halfway between the Shuttle and the subsatellite.

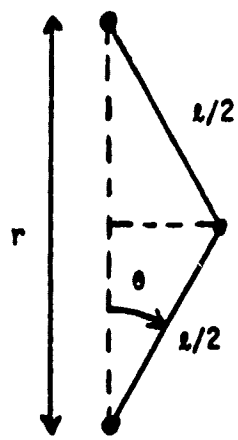

Figure 9.

The distance r between the ends of the wire is

$$r = 2\left(\frac{\ell}{2} - \frac{\ell}{2}\cos\theta\right) = \ell - \ell\cos\theta$$

The radial velocity is

$$\dot{r} = \ell \sin\theta\,\dot{\theta},$$

And the radial acceleration is

$$\ddot{r} = \ell(\cos\theta\,\dot{\theta}^2 + \sin\theta\,\ddot{\theta}) \quad .$$

If we assume

$$\theta = \theta_o \sin\omega t$$

from which we have

$$\dot{\theta} = \theta_o\,\omega\cos\omega t \quad ,$$

and

$$\ddot{\theta} = -\theta_o\omega^2 \sin\omega t \quad ,$$

then

$$\ddot{r} = \ell(\cos\theta\,\theta_o^2\,\omega^2\cos^2\omega t - \sin\theta\,\theta_o\,\omega^2\sin\omega t)$$

$$= \ell\,\theta_o\,\omega^2\,(\theta_o\cos\theta\cos^2\omega t - \sin\theta\sin\omega t) \quad .$$

For small values of θ_o, the factor in parentheses can be simplified. Making the substitution $\theta = \theta_o \sin\omega t$ we have

$$\ddot{r} = \ell\theta_o\omega^2\,(\theta_o\cos[\theta_o\sin\omega t]\cos^2\omega t$$

$$- \sin[\theta_o\sin\omega t]\sin\omega t)$$

$$\approx \ell\theta_o\omega^2\,(\theta_o\cos^2\omega t - \theta_o\sin^2\omega t)$$

Using the identity $\cos 2\omega t = \cos^2\omega t - \sin^2\omega t$ we have the approximate equation

$$\ddot{r} \approx \ell\,\theta_o^2\,\omega^2\cos 2\omega t \quad .$$

From the equation of motion for transverse oscillations,

$$m_w \frac{\ell}{2} \ddot{\theta} = -2T\theta \quad ,$$

we see that natural frequency is $\omega = \sqrt{4T/m_w \ell}$ where m_w is the wire mass and T is the wire tension.

3.7 Tension Variations Due to Longitudinal Oscillations

The dominant source of tension variations in generally longitudinal oscillations of the subsatellite at the end of the tether. The natural frequency ω of the oscillations is

$$\omega = \sqrt{k/m}$$

where m is the mass of the subsatellite and k is the stiffness of the tether. The stiffness k is

$$k = EA/\ell$$

where E is the elasticity of the tether material, A is the cross sectional area and ℓ is the tether length. Neglecting tether mass, the oscillations occur about the center of mass of the Shuttle plus subsatellite, so that one can use for ℓ the distance from the subsatellite to the center of mass.

3.8 Transverse and Longitudinal Propagation Velocities

Transverse acceleration of the subsatellite at the end of the tether generates a transverse wave which travels down the wire at a speed determined by the tether tension and mass per unit length. The propagation speed v_T is

$$v_T = \sqrt{T/\rho A}$$

where T is the tension, ρ is the density of the tether material, and A the cross sectional area. When there are substantial coriolis forces due to acceleration of the subsatellite, the tension may be much greater than the equilibrium value. After deceleration or payload release, the tension may be very low.

The velocity v_ℓ for propagation of stress along the tether is

$$v_\ell = \sqrt{E/\rho}$$

where E is the elasticity of the tether material and ρ is the density. For kevlar with density 1.44 g/cc and Young's modulus 7 x 10" dynes/cm^2 the speed of sound is about 7 x 10^5 cm/sec. There will therefore be a delay in propagating tension changes from one end of the tether to the other.

3.9 Coriolis Forces In-Plane and Out-of-Plane

For small angles, the equilibrium wire tension is given by

$$T = m\,(r\dot{\phi}^2 + r\dot{\theta}^2 + 2r\dot{\theta}\dot{\gamma} + 3r\dot{\gamma}^2) \quad .$$

There is an asymmetry between in-plane and out-of-plane launches when the payload is accelerated by thrusters. There is a term $2r\dot{\theta}\dot{\gamma}$ which arises because the in-plane angular velocity is parallel to the orbital angular velocity. There is no corresponding term for the out-of-plane angular velocity.

3.10 Coupling Between In-Plane and Out-of-Plane Oscillations

Out-of-plane launches using thrusters to accelerate the payload produce a component of motion in the in-plane direction because of coupling between the variables. In-plane launches produce no out-of-plane motion as long as there is no initial out-of-plane oscillation. The reasons for this behavior can be seen from the equations of motion. The coupling terms for the out-of-plane acceleration ($\ddot{\phi}$) are

$$r \sin\phi \cos\phi\,[\dot{\theta} + \dot{\gamma}]^2$$

and

$$2\dot{r}\dot{\phi} \quad .$$

If ϕ is zero, then the first term is zero for all values of $\dot{\theta}$ because of the sin ϕ factor. If ϕ is zero then $\dot{\phi}$ is of course also zero so that the term $2\dot{r}\dot{\phi}$ causes no out-of-plane motion. The coupling terms for the in-plane acceleration ($\ddot{\theta}$) are

$$2\,(\dot{\theta}+\dot{\gamma})\,\dot{r}\cos\phi$$

and

$$-2\,(\dot{\theta}+\dot{\gamma})\,r\,\dot{\phi}\sin\phi$$

The second term will produce an in-plane acceleration, whenever there is an out-of-plane velocity except at the point where the out-of-plane angle is zero. In addition if there is a radial velocity, the first term will contribute to the in-plane acceleration.

3.11 Reel Control Algorithms for Payload Release

The algorithms described in this section are designed for releasing a payload at the end of a long tether in a stable manner. We assume that the payload has been deployed to the desired distance from the Shuttle and stabilized in a vertical configuration. The objective is to release the payload in a manner that will not cause recoil of the remaining mass and loss of tension in the tether. A relatively simple approach is to use the reel motor to induce a longitudinal oscillation of the end mass, and release the payload when the tension is at its minimum and close to the equilibrium value for the remaining mass.

The initial study of this technique was done using a small program which integrates the motion of two bodies connected by a massless tether. The action of the reel motor is simulated by having the natural length ℓ_0 of the elastic wire be a function of time according to the equation

$$\ell_0 = \ell_c, \quad t < t_0 \tag{31a}$$

$$\ell_0 = \ell_c - \Delta\ell \sin \omega (t - t_0), \quad t_0 < t < t_f \tag{31b}$$

$$\ell_0 = \ell_c - \Delta\ell \sin \omega (t_f - t_0), \quad t > t_f \tag{31c}$$

The constant ω is chosen to be the same as the natural frequency for longitudinal oscillations of the end mass in order to maximize the induced oscillation. By choosing $t_f - t_0$ equal to one half cycle, the effect is to pull the end mass toward the Shuttle during the first quarter cycle and then return the wire to its original length during the second quarter of a cycle before the end mass has a chance to return to its original position.

Equation (31) has discontinuities in the wire velocity at t_0 and t_f which tend to excite wire oscillations. An alternative to specifying length vs. time is to specify tension vs. time. We can use a tension control law of the form

$$T = T_0, \qquad t < t_0 \tag{32a}$$

$$T = T_0 + \Delta T \sin \omega (t - t_0) \qquad t_0 < t < t_f \tag{32b}$$

$$T = T_0 + \Delta T \sin \omega (t_f - t_0) \qquad t > t_f \tag{32c}$$

When equation (31) is used, the minimum tension occurs at one half cycle. For equation 32, the minimum tension occurs at 3/4 of a cycle. Therefore, ω in equation (32) has been set so that the period is 2/3 of that used in equation (31). There is considerably less excitation of wire oscillations using tension control. This should make it possible to predict and control the tension at the time of release of a payload more accurately.

More work needs to be done to develop algorithms for damping wire oscillations during reeling operations and payload releases.

3.12 Other Methods for Avoiding Loss of Tension After Payload Release

Section 3.11 describes a maneuver for avoiding loss of tension due to rebound after release of a heavy payload. In addition to the longitudinal oscillation of the payload after release there will be stress waves propagating along the wire. It should be possible to develop a control algorithm for the reel motor which will damp out these oscillations. When the end mass is accelerated by thrusters, coriolis effects will tend to stretch the wire, increasing the tension and causing energy to be stored in the wire which can cause rebound when the payload is released and the remaining mass decelerated. The direction of the thrust could be controlled so as to provide a longitudinal component to cancel the coriolis forces. This longitudinal component could also be used to compress the wire to the point where the wire tension is at the value anticipated after payload release. Deceleration after release will again reduce the equilibrium tension value. The thrust could be directed so as to bring the wire to an equilibrium condition without loss of tension. Additional work would be required to develop algorithms for controlling the thrusters so as to avoid loss of tension in the wire.

Another possibility is to have a reel on the subsatellite that could deploy some wire to reduce the tension when a payload is released. The amount of wire required would be on the order of the stretch in the wire which could be a kilometer or more. The shuttle could also release wire to reduce the tension. It would be necessary to anticipate the release because of the propagation delay along the wire.

3.13 Long vs. Short Tether Launcher

In a short tether, the equilibrium tension due to the gradient of the gravitational and centrifugal forces is small. If the end mass is accelerated in order to launch a payload the centrifugal forces generated may be large

compared to the equilibrium tension so that the tension goes through a large dynamic range. The angular velocity and angular displacement during the acceleration and deceleration phases may also be large. Therefore the velocities that can be achieved without generating instabilities are rather limited. Only a small velocity is required to start the end mass circling around the Shuttle.

In a long tether the equilibrium tension is larger and the centrifugal forces are smaller so that the dynamic range of the tension is smaller. The stretch of the wire is larger so that more radial displacement can be accomodated without loss of tension in the tether. The angular displacement corresponding to a fixed lateral displacement decreases with tether length. The linear displacement and velocity of natural pendulum oscillations of the tether is larger, so that larger subsatellite velocities are required to generate instabilities. The mass of the tether itself is larger compared to the mass of the subsatellite, and tends to be a stabilizing factor since more energy is required to excite motions of the tether.

Considering all of the above factors, it would appear that long tethers are more effective and stable than short tethers. A short tether would probably have to circle the Shuttle to achieve large launch velocities.

3.14 Cases Run

Various cases have been run to study the use of the tether as a launcher. These have been done with andwithout thrusters, with short and long tethers, for in-plane and out-of-plane launches, with slack tethers, and with techniques for keeping the wire in tension. The details of the runs are described in Monthly Reports 8 through 13 dated June through November 1980.

Some initial runs were done with damping between all of the mass points representing the wire. The behavior of such a system is significantly different from a purely elastic wire because longitudinal oscillations of the wire

and end mass are suppressed. In practice, damping could be implemented at one or both ends of the wire. Therefore, most runs have been done with purely elastic forces or special control laws or damping at the ends.

Because of the representation of the wire by discrete masses, the Skyhook program is not well suited to studying slack tethers. In a test run where the thrusters were fired in a direction such that the wire goes slack, tension spikes resulted when the individual mass points came back into tension. Increasing the number of mass points might help give more reasonable results but it is difficult to conceive of any good way of modelling a slack tether. Effort has been concentrated on devising methods of avoiding loss of tension in the wire.

Runs have been done to verify the formulas and principles discussed in the previous sections. The expression for tension variations due to transverse wire oscillations is easily verified only when damping is used to suppress longitudinal oscillations. Without damping, longitudinal oscillations of the subsatellite at the end of the wire dominate the behavior of the tension. Launches using in-plane thrusters show no out-of-plane motion and larger coriolis forces because of the addition of the tether and orbital angular velocities. Out-of-plane launches have lower coriolis forces and a slight in-plane motion developes because of coupling terms in the equations of motion. The excitation of longitudinal oscillations of the subsatellite and transverse wire oscillations is in reasonable agreement with the formulas developed. Runs using thrusters with short tethers show the large range of tension variation and potential problems with unstable wire dynamics discussed in the section on long vs. short tethers.

Test runs indicate that the release of a heavy payload, either in the static case, or after acceleration by thrusters, results in loss of wire tension due to rebound unless special techniques are used to deal with the problem.

Transverse acceleration of the payload induces a radial oscillation because of coriolis forces. In one test run, release of the payload was delayed until the minimum of the tension cycle caused by the radial oscillation. This procedure avoided loss of tension, but larger transverse wire motion resulted because of the longer distance travelled by the end mass.

In order to investigate the behavior of the wire when thrusters are used some simulations have been done with five masses, three of which represent the wire. A two metric ton subsatellite at the end of a 200 km wire is accelerated to 200 m/sec in 20 seconds and decelerated from 20 to 40 seconds. Figure 11a shows the behavior of the tension in each of the wire segments vs. time. Figure 10 shows the numbering of the mass points.

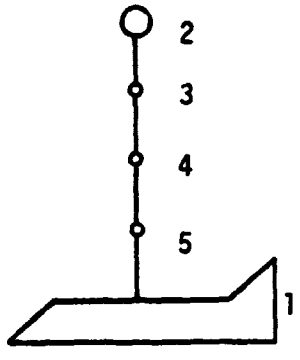

Figure 10.

The tension plotted for each mass point is the tension between that mass and the next higher numbered mass point. For the last mass, #5, it is the tension to the Shuttle which is mass #1. The initial conditions are set up so that the tension is equal between all the mass points. This is not an equilibrium condition since the tension is greatest near the Shuttle and smallest near the subsatellite. The long period variation of the tension is due to the longitudinal oscillation of the subsatellite induced by the coriolis forces during acceleration and deceleration. The short period variation results

from longitudinal oscillations of the wire masses. The damping coefficient has been reduced to a negligible value in this run so that the longitudinal oscillations are not suppressed. There was no release of the subsatellite and no loss of tension in the wire.

Figure 11b shows the in-plane motion of the wire. The in-plane axis is expanded by about a factor of 50 relative to the radial axis. As the subsatellite at the top is accelerated it generates a transverse wave which travels down the wire to the Shuttle at the bottom.

Runs have been done to study the release of a heavy paylaod without thrusters using reel control algorithms to avoid loss of tension in the tether. The simulations use 5 mass points, three of which represent the wire. Equilibrium initial conditions are set up for a 10 metric ton payload at the end of an 80 km wire. The length control algorithm described in Section 3.11 is used with t_o = 10 sec and t_f = 195 seconds.

The tension as a function of time is shown in Figure 12(a). The tension is constant for the first ten seconds. If the speed of sound is about 7 km/sec in kevlar the propagation delay for stress along an 80 km tether is about 11.5 seconds. This seems to be in approximate agreement with the delay time seen in the plot. The maneuver sets up stress waves along the tether which cause tension fluctuations. After release of the payload, although the average tension is near the desired value, wire oscillations cause loss of tension at various points along the wire.

The potential tether materials being considered for the Skyhook system all have low hysteresis, so that there would be little damping of stress waves along the wire. However, since there is strong compling between the action of the reel motor and the longitudinal oscillations, it should be possible to damp longitudinal oscillations by a suitable tension or rate control law at the end of the wire. A run has been done with the Skyhook program to test

the principle that longitudinal oscillations can be controlled by introducing damping at the end of the wire. The run described in Figure 12(a) has been repeated with damping introduced between the subsatellite and the wire mass adjacent to it. There was no damping in the other three wire segments, and equation (31) was used to control the natural length of the wire segment next to the Shuttle. The tension as a function of time is shown in Figure 12(b). The wire oscillations induced by equation (31) have been damped out, and the oscillations induced by the payload release at 195 seconds are also reduced with time. There is no loss of tension.

In cases where the tether length and mass are larger and the payload is smaller, the effect of wire dynamics is increased. A run has been done using equation (31) for a 200 km tether with a two ton payload. The tension vs. time is shown in Figure 13(a). The tension is constant for the first ten seconds. The propagation delay should be about 28.7 seconds for stress waves along the tether. The tension variations along the tether are of larger relative amplitude and longer period than in Figure 12(a).

Equation (31) has discontinuities in the wire velocity at t_o and t_f which tend to excite wire oscillations. An alternative to specifying length vs. time is to specify tension vs. time. A run has been done using the tension control law given in Section 3.11. The tension vs. time is shown in Figure 13(b). There is considerably less excitation of wire oscillations than in Figure 13(a). This should make it possible to predict and control the tension at the time of release of a payload more accurately.

More work needs to be done to develop algorithms for damping wire oscillations during reeling operations and payload releases.

3.15 Conclusions

The tether appears to be a useful device for transferring payloads between orbits in an economical manner. In the case of release of a payload without acceleration by thrusters, the tether and the remaining mass at the end recoil resulting in loss of tension. This tension loss can be prevented and longitudinal wire oscillations can be damped using the tether reel motor. In the case of acceleration of the end mass by thrusters, both longitudinal and transverse wire motions are set up. Some techniques for avoiding loss of tension have been tested and other possible techniques have been discussed. Further work needs to be done to develop appropriate algorithms. Long tethers appear to be more stable than short tethers. As a result of the elasticity of the tether, the subsatellite is almost semi-free to maneuver at the end of a long tether without loss of tension.

FIGURE CAPTIONS

Figure 11(a). Tension vs. time for each wire segment when the payload is accelerated by a thruster.

Figure 11(b). In-plane wire configuration vs. time when the payload is accelerated by a thruster.

Figure 12(a). Tension vs. time in each wire segment using the length control algorithm. The tether is 80 km long and the subsatellite is 10 tons.

Figure 12(b). Tension vs. time in each wire segment using the length control algorithm with damping in the wire segment next to the subsatellite.

Figure 13(a). Tension vs. time in each wire segment using the length control algorithm. The tether is 200 km long and the subsatellite is two tons.

Figure 13(b). Tension vs. time in each wire segment using the tension control algorithm.

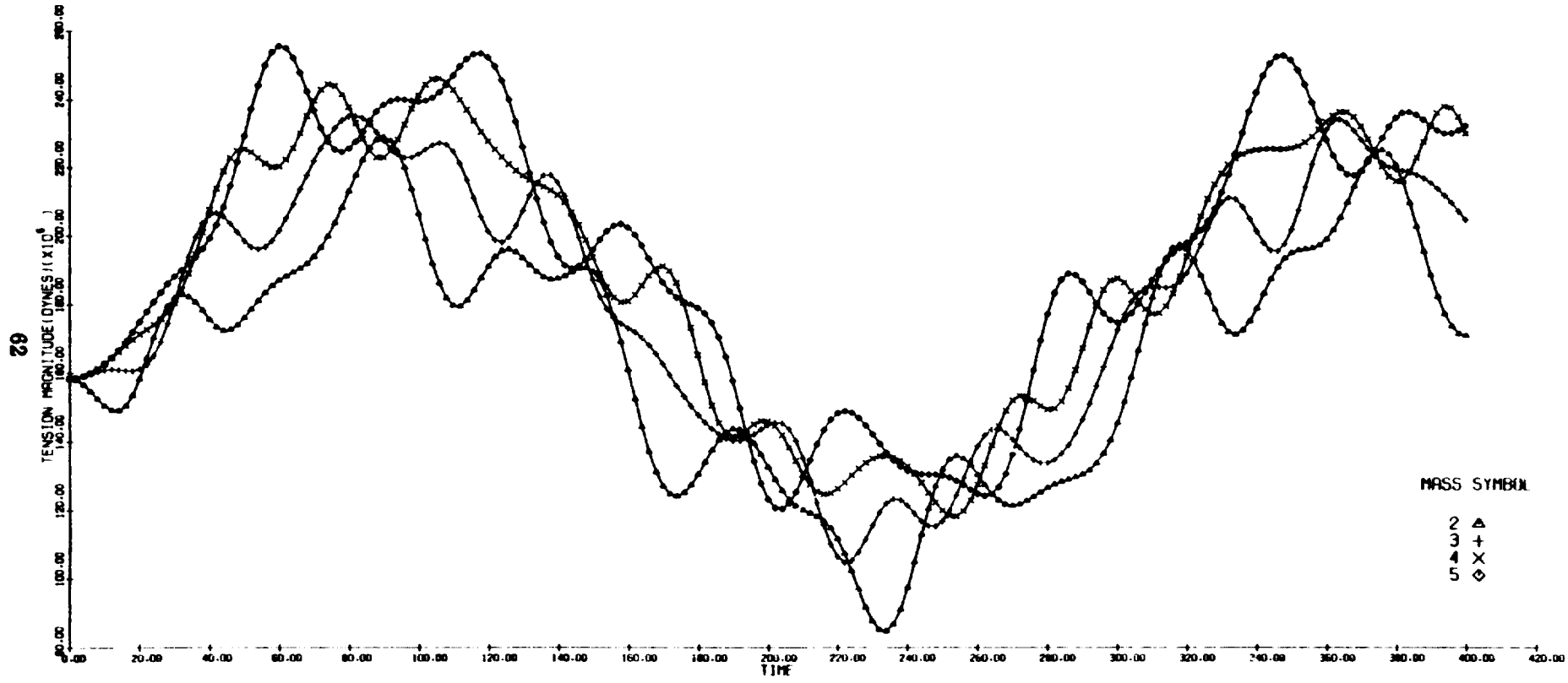

Figure 11a.

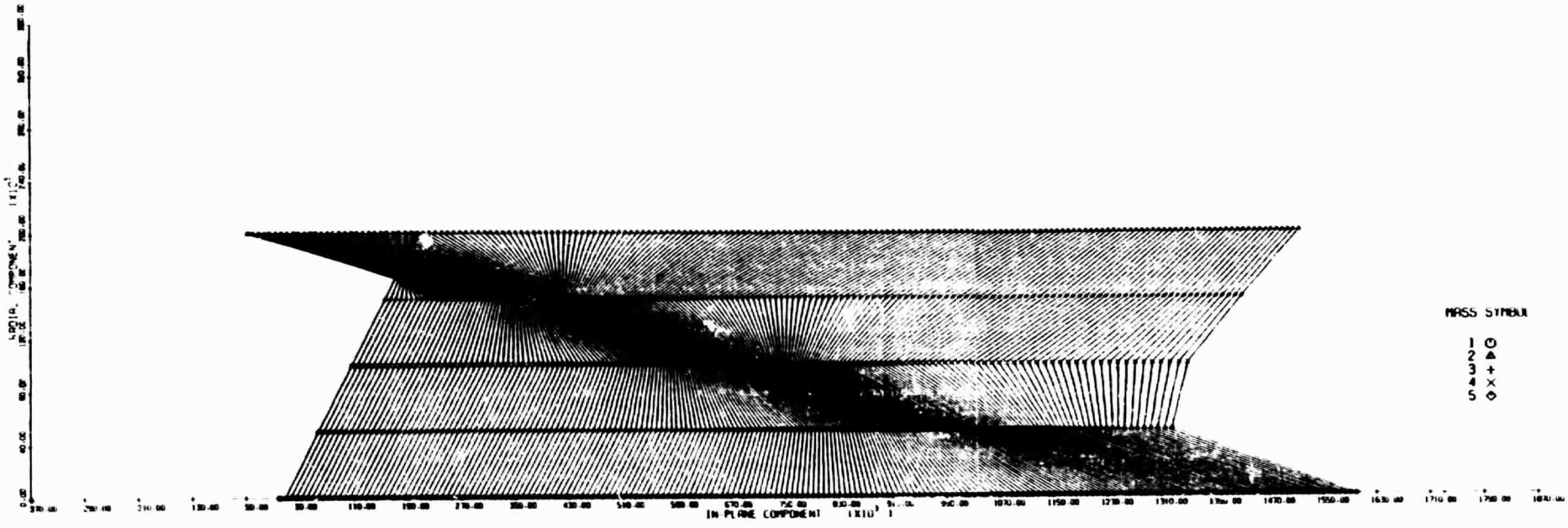

Figure 11b.

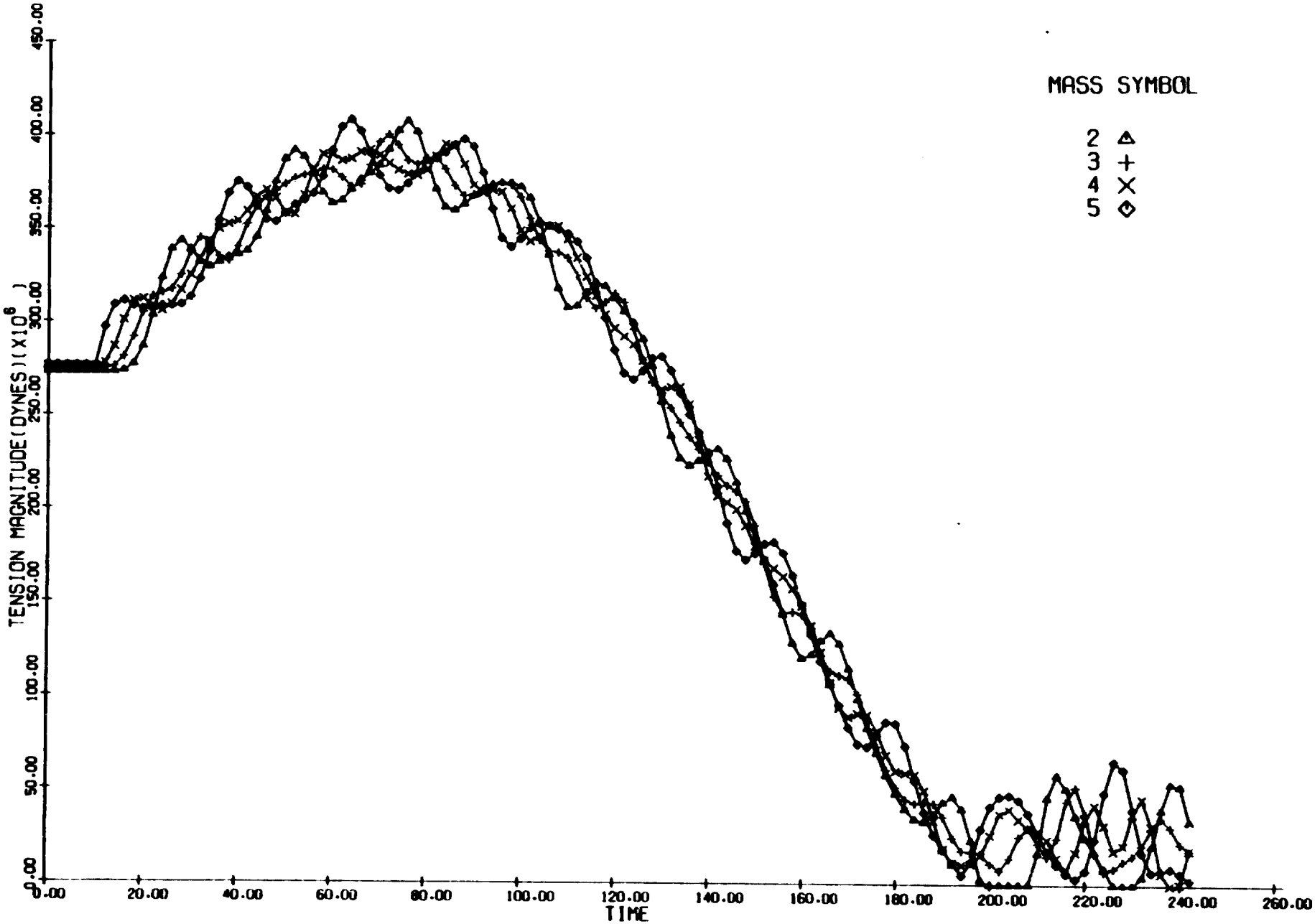
MASS SYMBOL
2
3
4
5
TENSION MAGNITUDE(DYNES)((X10^6)
TIME
0.00
50.00
100.00
150.00
200.00
250.00
300.00
350.00
400.00
450.00
0.00
20.00
40.00
60.00
80.00
100.00
120.00
140.00
160.00
180.00
200.00
220.00
240.00
260.00

Figure 12a.

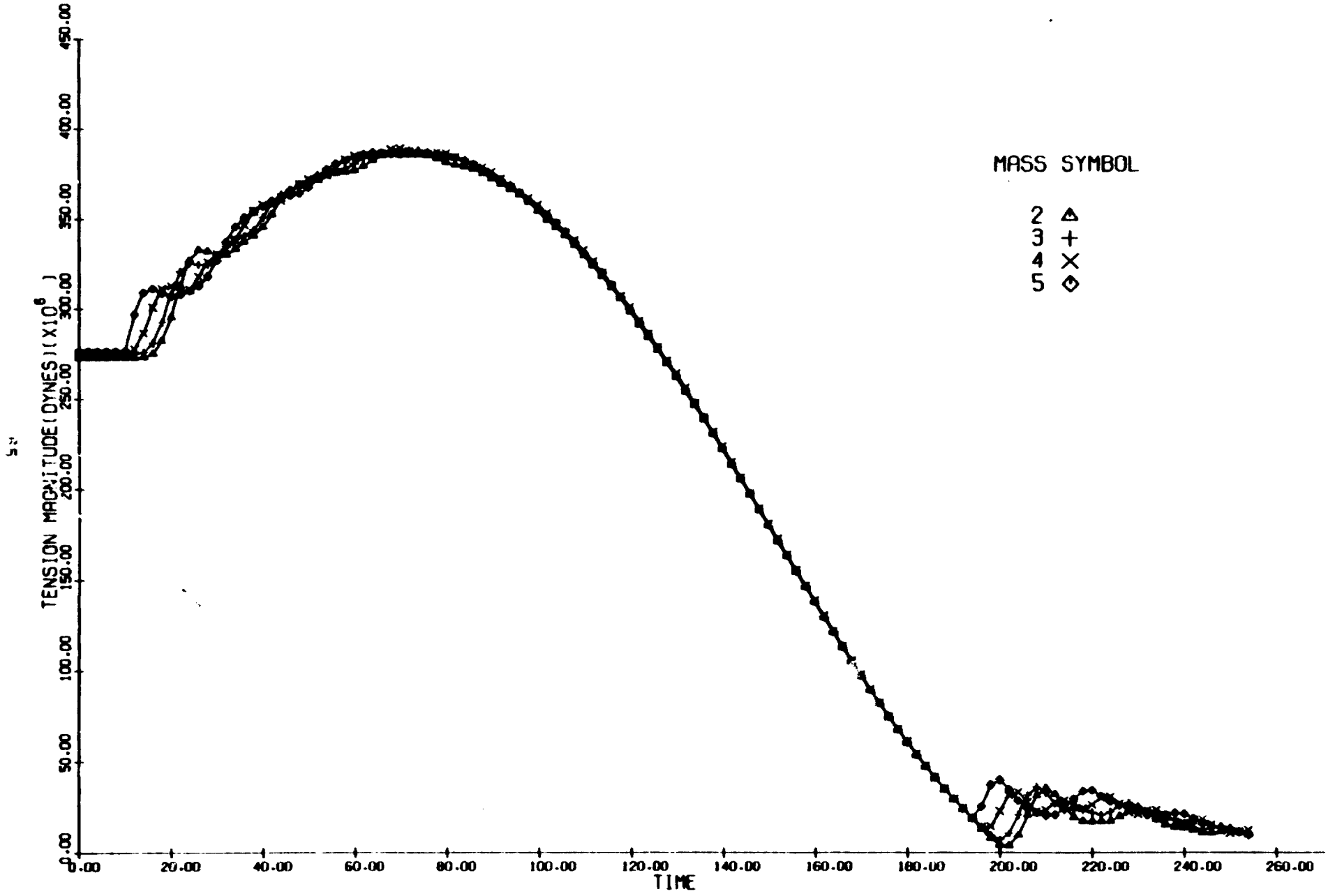
MASS SYMBOL
2 △
3 +
4 X
5 ◇
TENSION MAGNITUDE(DYNES)(X10^6)
TIME
0.00
50.00
100.00
150.00
200.00
250.00
300.00
350.00
400.00
450.00
0.00
20.00
40.00
60.00
80.00
100.00
120.00
140.00
160.00
180.00
200.00
220.00
240.00
260.00

Figure 12b.

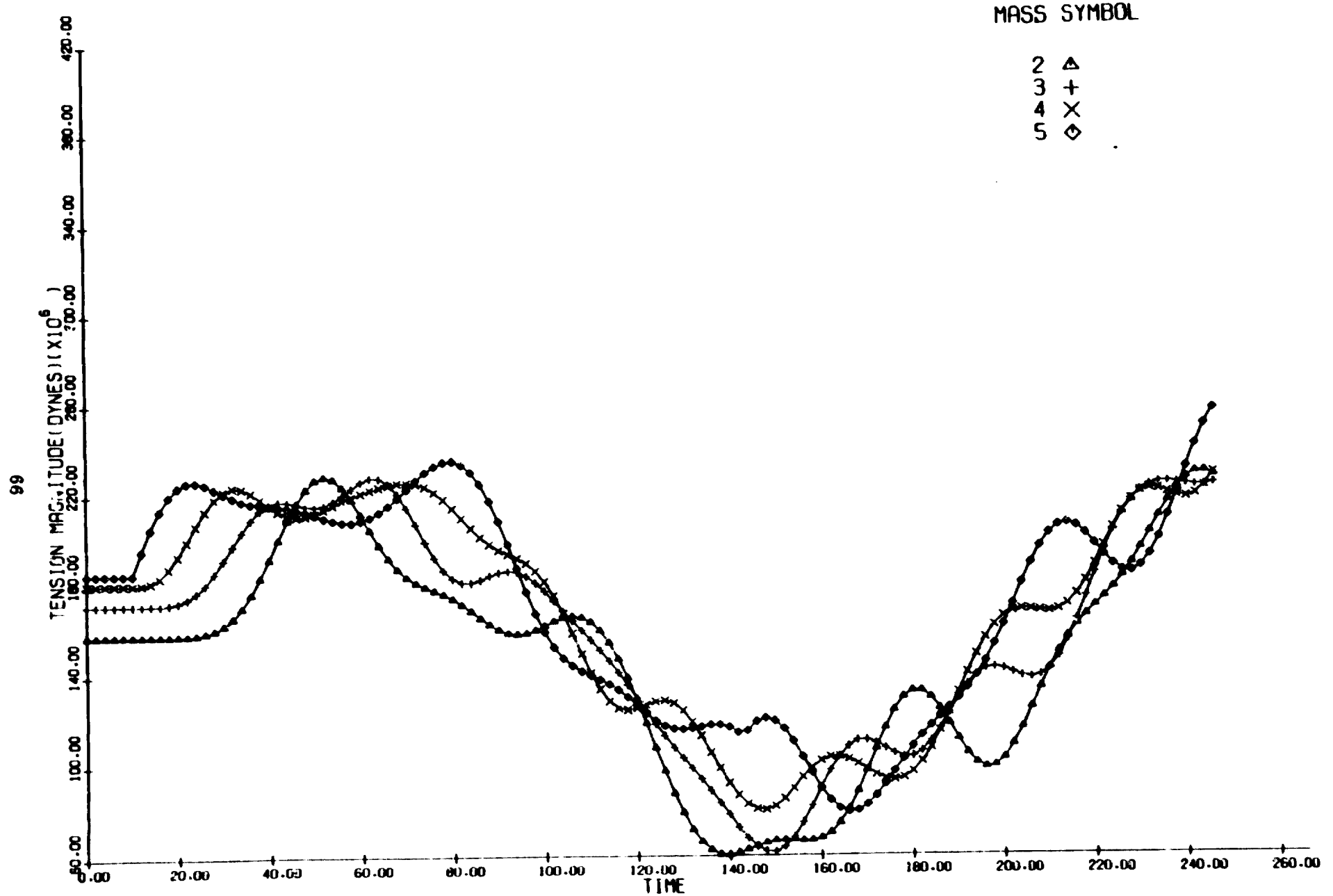
MASS SYMBOL
2
3
4
5
TENSION MAGNITUDE(DYNES)(X10^6)
TIME
0.00
20.00
40.00
60.00
80.00
100.00
120.00
140.00
160.00
180.00
200.00
220.00
240.00
260.00
60.00
100.00
140.00
180.00
220.00
260.00
300.00
340.00
380.00
420.00

Figure 13a.

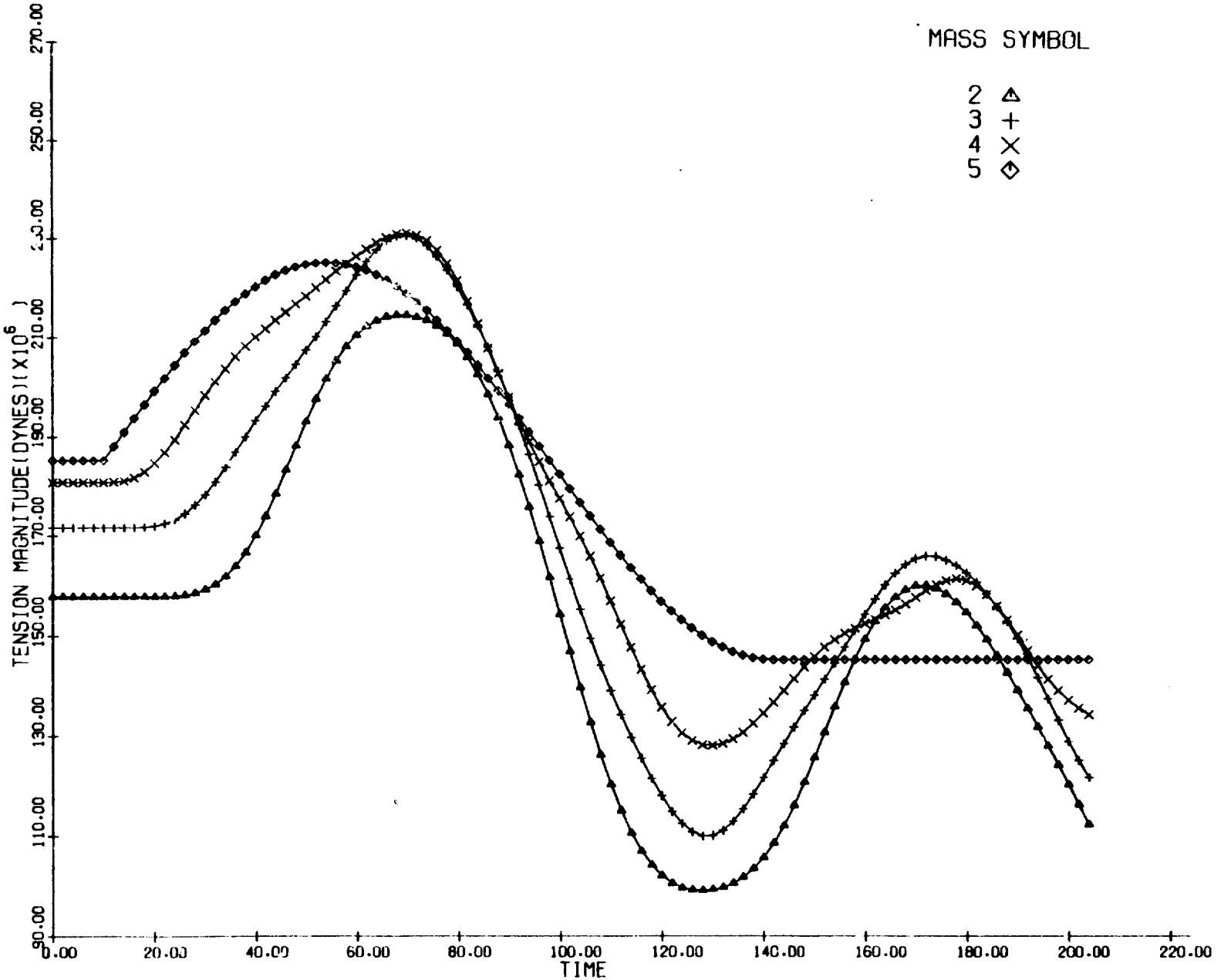
MASS SYMBOL
2
3
4
5
TENSION MAGNITUDE(DYNES)(X10^6)
270.00
250.00
230.00
210.00
190.00
170.00
150.00
130.00
110.00
90.00
0.00
20.00
40.00
60.00
80.00
100.00
120.00
140.00
160.00
180.00
200.00
220.00
TIME

Figure 13b.

Appendix A

General Equations of Motion

In this section, the general equations of motion are derived for a tether system modelled as a mass m at the end of a massless straight tether which applies a tension force on the mass m in the direction of the Shuttle. The Shuttle is assumed to move at constant angular velocity in the x-y plane as shown in Figure A1.

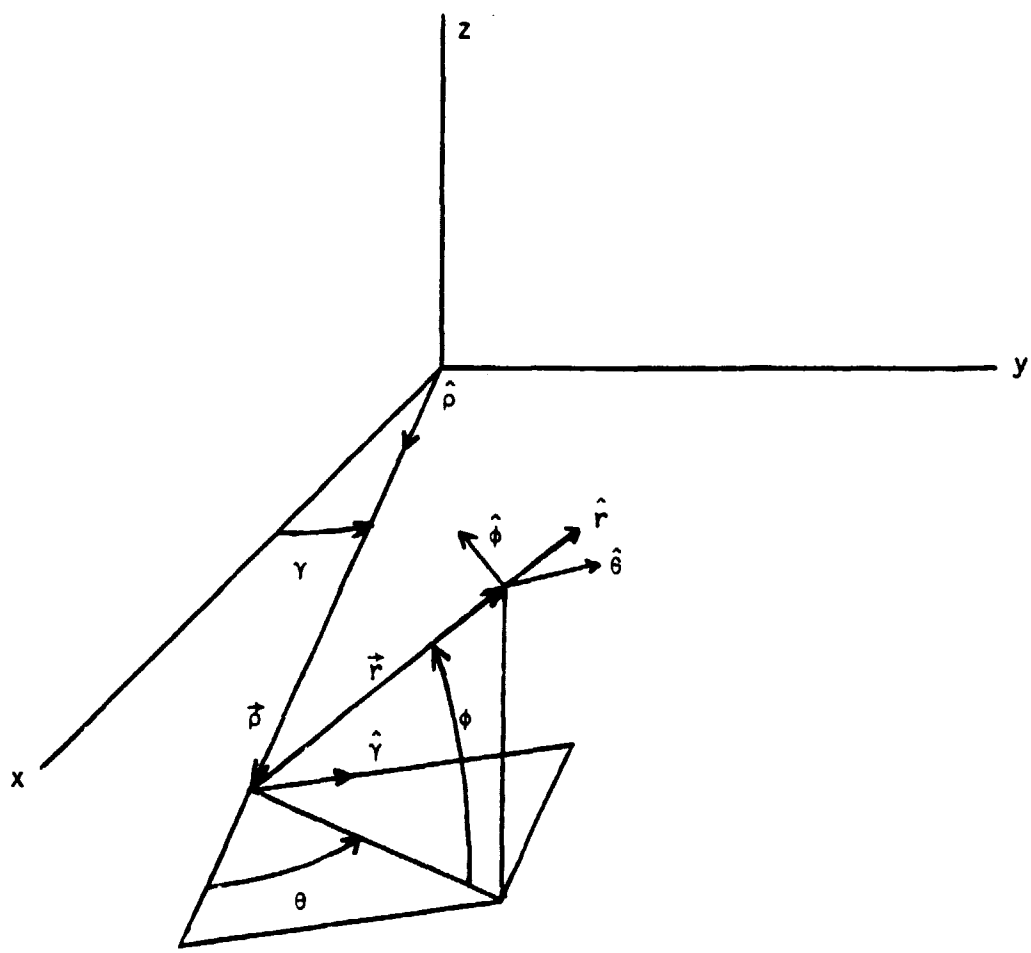

The position of the Shuttle is given by the vector $\vec{\rho}$. In cases where the mass m is not negligible compared to the mass of the Shuttle, the Shuttle does not move with constant angular velocity. In this case, the vector $\vec{\rho}$ can be used

to define the position of the center of the system which does move at constant angular velocity. The position of the mass m relative to the center of the system is given by the vector $\vec{r}$. The position $\vec{P}$ of mass m relative to the center of the earth is

$$\vec{P} = \vec{\rho} + \vec{r} \tag{A1}$$

The equation of motion of mass m is

$$\vec{F} = m \ddot{\vec{P}} \tag{A2}$$

where $\vec{F}$ is the total force on the system. The force $\vec{F}$ is given by

$$\vec{F} = \vec{F}_g + \vec{F}_e \tag{A3}$$

where $\vec{F}_g$ is the gravitational force and $\vec{F}_e$ is all other forces such as the tension in the tether, atmospheric drag, etc. Differentiating equation (A1) twice gives

$$\ddot{\vec{P}} = \ddot{\vec{\rho}} + \ddot{\vec{r}} \tag{A4}$$

Since ρ and $\dot{\gamma}$ are both constant, $\ddot{\vec{\rho}}$ is given by the usual expression for the centrifugal acceleration, and we can write

$$\ddot{\vec{\rho}} = -\rho\dot{\gamma}^2 \hat{\rho} \tag{A5}$$

where $\hat{\rho}$ is a unit vector in the direction of $\vec{\rho}$. The second part of equation (A4) can be evaluated as

$$\begin{aligned} \ddot{\vec{r}} &= \frac{d^2}{dt^2}(r\hat{r}) = \frac{d}{dt}(\dot{r}\hat{r} + r\dot{\hat{r}}) \\ &= \ddot{r}\hat{r} + 2\dot{r}\dot{\hat{r}} + r\ddot{\hat{r}} \end{aligned} \tag{A6}$$

In Figure A1, the unit vectors $\hat{r}$, $\hat{\theta}$, and $\hat{\phi}$ form an orthogonal coordinate system. The derivative of any of these unit vectors is perpendicular to that unit vector and must therefore be in the plane defined by the other two unit vectors. This fact can be used to simplify the evaluation of equation (A6). From Figure A1 we have the following expressions for the unit vectors.

$$\hat{r} = \cos\phi\cos\theta\hat{\rho} + \cos\phi\sin\theta\hat{\gamma} + \sin\phi\hat{k} \tag{A7a}$$

$$\hat{\theta} = -\sin\theta\hat{\rho} + \cos\theta\hat{\gamma} \tag{A7b}$$

$$\hat{\phi} = -\sin\phi\cos\theta\hat{\rho} - \sin\phi\sin\theta\hat{\gamma} + \cos\phi\hat{k} \tag{A7c}$$

We need to differentiate equation (A7a) to obtain an expression for $\dot{\hat{r}}$ in equation (A6). In doing the differentiation we use the relations

$$\dot{\hat{\rho}} = \dot{\gamma}\,\hat{\gamma} \tag{A8a}$$

$$\dot{\hat{\gamma}} = -\dot{\gamma}\,\hat{\rho} \tag{A8b}$$

and

$$\dot{\hat{k}} = 0 \tag{A8c}$$

to obtain the result

$$\begin{aligned}\dot{\hat{r}} = {} & -\sin\phi\cos\theta\dot{\phi}\hat{\rho} - \cos\phi\sin\theta\dot{\theta}\hat{\rho} + \cos\phi\cos\theta\dot{\gamma}\hat{\gamma} \\ & -\sin\phi\sin\theta\dot{\phi}\hat{\rho} + \cos\phi\cos\theta\dot{\theta}\hat{\gamma} - \cos\phi\sin\theta\dot{\gamma}\hat{\rho} \\ & +\cos\phi\dot{\phi}\hat{k}\end{aligned} \tag{A9}$$

Equation (A9) must be a linear combination of equations (A7b) and (A7c). By inspection we see that the terms in each column of equation (A9) are multiples of either $\hat{\theta}$ or $\hat{\phi}$. Therefore we have

$$\begin{aligned}\dot{\hat{r}} &= \dot{\phi}\hat{\phi} + \cos\phi\dot{\theta}\hat{\theta} + \cos\phi\dot{\gamma}\hat{\theta} \\ &= \dot{\phi}\hat{\phi} + \cos\phi(\dot{\theta}+\dot{\gamma})\hat{\theta}\end{aligned} \tag{A10}$$

Differentiating equation (A10) to obtain $\ddot{\hat{r}}$ needed in equation (A6) we have

$$\begin{aligned}\ddot{\hat{r}} = {} & \ddot{\phi}\hat{\phi} + \dot{\phi}\dot{\hat{\phi}} - \sin\phi\dot{\phi}(\dot{\theta}+\dot{\gamma})\hat{\theta} + \cos\phi\ddot{\theta}\hat{\theta} \\ & + \cos\phi(\dot{\theta}+\dot{\gamma})\dot{\hat{\theta}}\end{aligned} \tag{A11}$$

To complete the derivation of equation (A11) we need $\dot{\hat{\theta}}$ and $\dot{\hat{\phi}}$. Differentiating equation (A7b) with the help of equation (A8), we have

$$\ddot{\hat{\theta}} = -\cos\theta\ddot{\theta}\hat{\rho} - \sin\theta\dot{\gamma}\dot{\hat{\gamma}}$$

$$- \sin\theta\dot{\theta}\dot{\hat{\gamma}} - \cos\theta\dot{\gamma}\dot{\hat{\rho}}$$

$$= -\cos\theta(\ddot{\theta}+\ddot{\gamma})\hat{\rho} - \sin\theta(\dot{\theta}+\dot{\gamma})\dot{\hat{\gamma}}$$

$$= -(\ddot{\theta}+\ddot{\gamma})(\cos\theta\hat{\rho} + \sin\theta\hat{\gamma}) \qquad \text{(A12)}$$

Equation (A12) must be a linear combination of equations (A7a) and (A7c). Since equation (A12) does not contain $\hat{k}$, the only possible combination is to multiply (A7a) by $\cos\phi$, multiply (A7c) by $\sin\phi$ and subtract to eliminate $\hat{k}$. Doing this we have

$$\cos\phi\dot{\hat{r}} - \sin\phi\dot{\hat{\phi}} =$$

$$\cos^2\phi\cos\theta\dot{\hat{\rho}} + \cos^2\phi\sin\theta\dot{\hat{\gamma}} + \cos\phi\sin\phi\dot{\hat{k}}$$

$$+ \sin^2\phi\cos\theta\dot{\hat{\rho}} + \sin^2\phi\sin\theta\dot{\hat{\gamma}} + \sin\phi\cos\phi\dot{\hat{k}}$$

$$= \cos\theta\dot{\hat{\rho}} + \sin\theta\dot{\hat{\gamma}} \qquad \text{(A13)}$$

Substituting equation (A13) into equation (A12) gives

$$\ddot{\hat{\theta}} = -(\ddot{\theta}+\ddot{\gamma})(\cos\phi\dot{\hat{r}} - \sin\phi\dot{\hat{\phi}}) \qquad \text{(A14)}$$

Next we evaluate $\ddot{\phi}$ which is needed in equation (A11). Differentiating equation (A7c) with the help of equation (A8) gives

$$\ddot{\hat{\phi}} = -\cos\phi\cos\theta\dot{\phi}\dot{\hat{\rho}} + \sin\phi\sin\theta\dot{\theta}\dot{\hat{\rho}} - \sin\phi\cos\theta\dot{\gamma}\dot{\hat{\gamma}}$$

$$- \cos\phi\sin\theta\dot{\phi}\dot{\hat{\gamma}} - \sin\phi\cos\theta\dot{\theta}\dot{\theta}\hat{\gamma} + \sin\phi\sin\theta\dot{\gamma}\dot{\hat{\rho}}$$

$$- \sin\phi\dot{\phi}\dot{\hat{k}} \qquad \text{(A15)}$$

Equation (A15) must be a linear combination of equations (A7a) and (A7c). By inspection we see that each column of equation (A15) is a multiple of either $\hat{r}$ or $\hat{\theta}$. Therefore equation (A15) can be written

$$\ddot{\hat{\phi}} = -\dot{\phi}\dot{\hat{r}} - \sin\phi\dot{\theta}\dot{\hat{\theta}} - \sin\phi\dot{\gamma}\dot{\hat{\theta}}$$

$$= -\dot{\phi}\dot{\hat{r}} - \sin\phi(\dot{\theta}+\dot{\gamma})\dot{\hat{\theta}} \qquad \text{(A16)}$$

Using equation (A14) and (A16) to complete the evaluation of equation (A11) we have

$$\begin{aligned}\ddot{\hat{r}} &= \ddot{\phi}\hat{\phi} + \dot{\phi}\,[-\dot{\phi}\hat{r} - \sin\phi(\dot{\theta}+\dot{\gamma})\hat{\theta}] - \sin\phi\dot{\phi}(\dot{\phi}+\dot{\gamma})\hat{\theta} \\ &\quad + \cos\phi\ddot{\theta}\hat{\theta} - \cos\phi(\dot{\theta}+\dot{\gamma})^2(\cos\phi\hat{r} - \sin\phi\hat{\phi}) \\ &= \hat{r}\,[-\dot{\phi}^2 - \cos^2\phi(\dot{\theta}+\dot{\gamma})^2] \\ &\quad + \hat{\theta}\,[-2\dot{\phi}\sin\phi(\dot{\theta}+\dot{\gamma}) + \ddot{\theta}\cos\phi] \\ &\quad + \hat{\phi}\,[\ddot{\phi} + \cos\phi\sin\phi(\dot{\theta}+\dot{\gamma})^2] \qquad \text{(A17)}\end{aligned}$$

Equation (A10) and (A17) are the results needed to evaluate equation (A16) for $\ddot{\vec{r}}$. Making the substitutions, we have

$$\begin{aligned}\ddot{\vec{r}} &= \ddot{r}\,\hat{r} \\ &\quad + 2\dot{r}\,[\dot{\phi}\hat{\phi} + \cos\phi(\dot{\theta}+\dot{\gamma})\hat{\theta}] \\ &\quad + r\,\Big\{\hat{r}\,[-\dot{\phi}^2 - \cos^2\phi(\dot{\theta}+\dot{\gamma})^2] \\ &\qquad + \hat{\theta}\,[-2\dot{\phi}\sin\phi(\dot{\theta}+\dot{\gamma}) + \ddot{\theta}\cos\phi] \\ &\qquad + \hat{\phi}\,[\ddot{\phi} + \cos\phi\sin\phi(\dot{\theta}+\dot{\gamma})^2]\Big\} \\ &= \hat{r}\,[\ddot{r} - r\dot{\phi}^2 - r\cos^2\phi(\dot{\theta}+\dot{\gamma})^2] \\ &\quad + \hat{\theta}\,[2\dot{r}\cos\phi(\dot{\theta}+\dot{\gamma}) - 2r\dot{\phi}\sin\phi(\dot{\theta}+\dot{\gamma}) + \ddot{\theta}r\cos\phi] \\ &\quad + \hat{\phi}\,[2\dot{r}\dot{\phi} + r\ddot{\phi} + r\cos\phi\sin\phi(\dot{\theta}+\dot{\gamma})^2]\end{aligned}$$

Equation (A5) gives $\ddot{\vec{\rho}}$ in terms of $\hat{\rho}$. We must express $\hat{\rho}$ in terms of $\hat{r}$, $\hat{\theta}$, and $\hat{\phi}$. The result can then be substituted along with equation (A18) into equation (A4) for $\ddot{\vec{P}}$. Equations (A7a, b, and c) form a set of simultaneous equations that can be solved for $\hat{\rho}$. Part of the work has already been done by eliminating $\hat{k}$ from equations (A7a, and c) to obtain equation (A13) which contains only $\hat{\rho}$ and $\hat{\gamma}$. Multiplying equation (A13) by $\cos\theta$ and equation (A7b) by $\sin\theta$ gives

$$\cos\theta(\cos\phi\hat{r} - \sin\phi\hat{\phi}) = \cos^2\theta\hat{\rho} + \cos\theta\sin\theta\hat{\gamma}$$

and

$$\sin\theta\hat{\theta} = -\sin^2\theta\hat{\rho} + \sin\theta\cos\theta\hat{\gamma}$$

which can be subtracted to yield

$$\cos\theta\cos\phi\hat{r} - \cos\theta\sin\phi\hat{\phi} - \sin\theta\hat{\theta} = \hat{\rho} \tag{A19}$$

Putting equation (A19) into equation (A5) gives

$$\begin{aligned}\ddot{\vec{\rho}} = &- \hat{r}\rho\dot{\gamma}^2\cos\theta\cos\phi \\ &+ \hat{\theta}\rho\dot{\gamma}^2\sin\theta \\ &+ \hat{\phi}\rho\dot{\gamma}^2\cos\theta\sin\phi\end{aligned} \tag{A20}$$

Adding equations (A18) and (A20) gives for equation (A4)

$$\begin{aligned}\ddot{\vec{P}} = &\hat{r}[\ddot{r}-r\dot{\phi}^2-r\cos^2\phi(\dot{\theta}+\dot{\gamma})^2-\rho\dot{\gamma}^2\cos\theta\cos\phi] \\ &+ \hat{\theta}[\ddot{\theta}r\cos\phi+2(\dot{\theta}+\dot{\gamma})(\dot{r}\cos\phi-r\dot{\phi}\sin\phi) + \rho\dot{\gamma}^2\sin\theta] \\ &+ \hat{\phi}[r\ddot{\phi}+2\dot{r}\dot{\phi}+r\cos\phi\sin\phi(\dot{\theta}+\dot{\gamma})^2 + \rho\dot{\gamma}^2\cos\theta\sin\phi]\end{aligned} \tag{A21}$$

Substituting equation (A21) into equation (A2) completes the derivation of the equations of motion for the variables r, θ, and ϕ. All forces $\vec{F}$ must be resolved along the unit vectors $\hat{r}$, $\hat{\theta}$, and $\hat{\phi}$. The tension force is in the $-\hat{r}$ direction and needs no further discussion. Atmospheric drag and other forces such as radiation pressure are not in a fixed direction and must be evaluated at each integration point. Equation (A7) gives the directions of the unit vectors $\hat{r}$, $\hat{\theta}$, and $\hat{\phi}$ as a function of $\hat{\rho}$, $\hat{\gamma}$, and $\hat{k}$. From Figure A1 we see that

$$\hat{\rho} = \cos\gamma\hat{i} + \sin\gamma\,\hat{j} \tag{A22a}$$

and

$$\hat{\gamma} = -\sin\gamma\hat{i} + \cos\gamma\hat{j} \tag{A22b}$$

Using equations (A7) and (A22), forces given in the $\hat{i}$, $\hat{j}$, $\hat{k}$ coordinate system can be resolved along $\hat{r}$, $\hat{\theta}$, and $\hat{\phi}$.

Neglecting higher harmonics, the gravitational force is always in the $-\vec{P}$ direction. Therefore it is useful to express the vector $\vec{P}$ in terms of $\hat{r}$, $\hat{\theta}$, and $\hat{\phi}$. Substituting equation (A19) into equation (A1) gives

$$\vec{P} = \hat{r}(r + \rho\cos\theta\cos\phi) - \hat{\theta}\rho\sin\theta - \hat{\phi}\rho\cos\theta\sin\phi \qquad \text{(A23)}$$

The gravitational force is

$$\vec{F}_g = -\frac{GMm}{P^3}\vec{P} \qquad \text{(A24)}$$

where P is the magnitude of $\vec{P}$. From equation (A23) we have

$$P^2 = r^2+2r\rho\cos\theta\cos\phi + \rho^2\cos^2\theta\cos^2\phi + \rho^2\sin^2\theta + \rho^2\cos^2\theta\sin^2\phi = r^2+2r\rho\cos\theta\cos\phi + \rho^2\sin^2\theta + \rho^2\cos^2\theta$$

or

$$P^3 = (r^2+2r\rho\cos\theta\cos\phi + \rho^2)^{3/2} \qquad \text{(A25)}$$

Substituting (A23) into (A24) gives

$$\vec{F}_g = -\frac{GMm}{P^3}\left[\hat{r}(r+\rho\cos\theta\cos\phi) - \hat{\theta}\rho\sin\theta - \hat{\phi}\rho\cos\theta\sin\phi\right] \qquad \text{(A26)}$$

Combining equations (A26), (A20), and (A3) into equation (A2) gives

$$\begin{aligned}\vec{F}_e = {} & m\hat{r}[\ddot{r}-r\dot{\phi}^2-r\cos^2\phi(\dot{\theta}+\dot{\gamma})^2-\rho\dot{\gamma}^2\cos\theta\cos\phi + GMP^{-3}(r+\rho\cos\theta\cos\phi)] \\ & + m\hat{\theta}[\ddot{\theta}r\cos\phi+2(\dot{\theta}+\dot{\gamma})(\dot{r}\cos\phi-r\dot{\phi}\sin\phi)+\rho\dot{\gamma}^2\sin\theta-GMP^{-3}\rho\sin\theta] \\ & + m\hat{\phi}[r\ddot{\phi}+2\dot{r}\dot{\phi}+r\cos\phi\sin\phi(\dot{\theta}+\dot{\gamma})^2+\rho\dot{\gamma}^2\cos\theta\sin\phi-GMP^{-3}\rho\cos\theta\sin\phi]\end{aligned} \qquad \text{(A27)}$$

with P given by equation (A25).

In cases where the tether length r is small compared to the radius of the orbit ρ, the exact equations of motion given in (A27) can be simplified by expanding the term P^{-3}. From equation (A25) we have

$$GMP^{-3} = GM(\rho^2 + 2r\rho\cos\theta\cos\phi + r^2)^{-3/2}$$
$$= GM\rho^{-3}(1 + 2\frac{r}{\rho}\cos\theta\cos\phi + \frac{r^2}{\rho^2})^{-3/2}$$
$$\approx GM\rho^{-3}(1 - 3\frac{r}{\rho}\cos\theta\cos\phi) \qquad \text{(A28)}$$

Using the relation $GM\rho^{-3} = \dot{\gamma}^2$ for a circular orbit, equation (A21) becomes

$$GMP^{-3} = \dot{\gamma}^2 - 3\frac{r}{\rho}\dot{\gamma}^2\cos\theta\cos\phi \qquad \text{(A29)}$$

Substituting (A29) into terms containing GMP^{-3} in (A27) and neglecting terms containing r/ρ, we have the relations

$$GMP^{-3}(r + \rho\cos\theta\cos\phi) \approx r\dot{\gamma}^2 + \dot{\gamma}^2\rho\cos\theta\cos\phi - 3r\dot{\gamma}^2\cos^2\theta\cos^2\phi \qquad \text{(A30a)}$$

$$GMP^{-3}\rho\sin\theta \approx \rho\dot{\gamma}^2\sin\theta - 3r\dot{\gamma}^2\cos\theta\cos\phi\sin\theta \qquad \text{(A30b)}$$

$$GMP^{-3}\rho\cos\theta\sin\phi \approx \dot{\gamma}^2\rho\cos\theta\sin\phi - 3r\dot{\gamma}^2\cos^2\theta\cos\phi\sin\phi \qquad \text{(A30c)}$$

Substituting equation (A30) into (A27) gives the approximate equations of motion

$$\vec{F}_e \approx$$
$$m\hat{r}[\ddot{r} - r\dot{\phi}^2 - r\cos^2\phi(\dot{\theta}+\dot{\gamma})^2 + r\dot{\gamma}^2 - 3r\dot{\gamma}^2\cos^2\theta\cos^2\phi]$$
$$+ m\hat{\theta}[\ddot{\theta}r\cos\phi + 2(\dot{\theta}+\dot{\gamma})(\dot{r}\cos\phi - r\dot{\phi}\sin\phi) + 3r\dot{\gamma}^2\cos\theta\cos\phi\sin\theta] \qquad \text{(A31)}$$
$$+ m\hat{\phi}[r\ddot{\phi} + 2\dot{r}\dot{\phi} + r\cos\phi\sin\phi(\dot{\theta}+\dot{\gamma})^2 + 3r\dot{\gamma}^2\cos^2\theta\cos\phi\sin\phi]$$

In equation (A31), ρ does not appear explicitly. It is used in calculating $\dot{\gamma}$, and it is assumed that r, θ, and ϕ are measured from a point at distance ρ from the center of the earth moving at constant angular velocity $\dot{\gamma}$. It is useful to derive the equations of motion for small values of θ and ϕ. The result is

$$\vec{F}_e \approx$$
$$m\hat{r}[\ddot{r} - r\dot{\phi}^2 - r\dot{\theta}^2 - 2r\dot{\theta}\dot{\gamma} - r\dot{\gamma}^2 + r\dot{\gamma}^2 - 3r\dot{\gamma}^2]$$
$$+ m\hat{\theta}[r\ddot{\theta} + 2(\dot{\theta}+\dot{\gamma})(\dot{r} - r\dot{\phi}\phi) + 3r\dot{\gamma}^2\theta]$$
$$+ m\hat{\phi}[r\ddot{\phi} + 2\dot{r}\dot{\phi} + r\phi(\dot{\phi}^2 + 2\dot{\theta}\dot{\gamma} + \dot{\gamma}^2) + 3r\dot{\gamma}^2\phi]$$

$$= m\hat{r}[\ddot{r} - r(\dot{\phi}^2+\dot{\theta}^2) - 2r\dot{\theta}\dot{\gamma} - 3r\dot{\gamma}^2]$$
$$+ m\hat{\theta}[r\ddot{\theta} + 2(\dot{\theta}+\dot{\gamma})(\dot{r}-r\dot{\phi}\phi) + 3r\dot{\gamma}^2\theta]$$
$$+ m\hat{\phi}[r\ddot{\phi} + 2\dot{r}\dot{\phi} + r\phi(\dot{\theta}^2+2\dot{\theta}\dot{\gamma}) + 4r\dot{\gamma}^2\phi] \qquad \text{(A32)}$$

If $\dot{\theta}$, $\dot{\phi}$ and $\dot{r}$ are also small, we obtain the simplest form of the equation namely,

$$\vec{F}_e \approx m\hat{r}(\ddot{r} - 3r\dot{\gamma}^2)$$
$$+ m\hat{\theta}(r\ddot{\theta} + 3r\dot{\gamma}^2\theta)$$
$$+ m\hat{\phi}(r\ddot{\phi} + 4r\dot{\gamma}^2\phi) \qquad \text{(A33)}$$

From equation (A33) we see that the equilibrium tension is $3mr\dot{\gamma}^2$, the natural frequency for in-plane oscillations is $\sqrt{3}\,\dot{\gamma}$ and the natural frequency for out-of-plane oscillations is $2\dot{\gamma}$.

Appendix B

Orbital Coordinate System

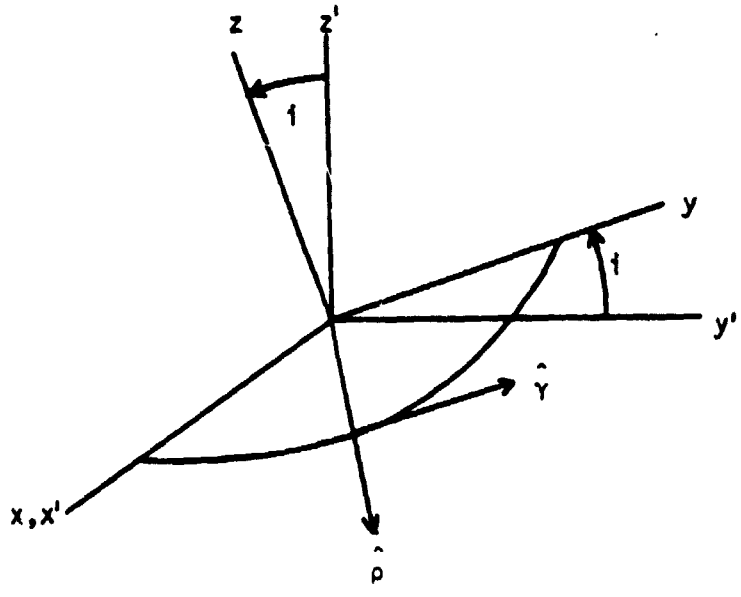

Figure B1

In Figure A1, the x and y axes are taken to be in the orbital plane, and the z-axis is the normal to the orbital plane. The unit vectors $\hat{\rho}$ and $\hat{\gamma}$ are given by equations (A22) in terms of the unit vectors along the axes. In Figure B1, the x'-y' axes are in the equatorial plane of the earth with the x' axis taken along the ascending node of the orbit. The two coordinate systems are related by a rotation about the x' axis through i where i is the inclination of the orbit. The unit vectors $\hat{i}$, $\hat{j}$ and $\hat{k}$ are related to the unit vectors $\hat{i}'$, $\hat{j}'$, and $\hat{k}'$ by the equations

$$\hat{i} = \hat{i}' \tag{B1a}$$

$$\hat{j} = \cos i\, \hat{j}' + \sin i\, \hat{k}' \tag{B1b}$$

$$\hat{k} = -\sin i\, \hat{j}' + \cos i\, \hat{k}' \tag{B1c}$$

Substituting equations (B1a and b) into equations (A22) gives

$$\hat{\rho} = \cos\gamma\,\hat{i}' + \sin\gamma\,(\cos i\,\hat{j}' + \sin i\,\hat{k}')$$

$$= \cos\gamma\,\hat{i}' + \sin\gamma\cos i\,\hat{j}' + \sin\gamma\sin i\,\hat{k}' \qquad \text{(B2a)}$$

$$\hat{\gamma} = -\sin\gamma\,\hat{i}' + \cos\gamma\,(\cos i\,\hat{j}' + \sin i\,\hat{k}')$$

$$= -\sin\gamma\,\hat{i}' + \cos\gamma\cos i\,\hat{j}' + \cos\gamma\sin i\,\hat{k}' \qquad \text{(B2b)}$$

Equations (B2a, B2b and B1c) define the unit vectors used in equation (A7) for an inclined orbit.

Appendix C

Initial Conditions

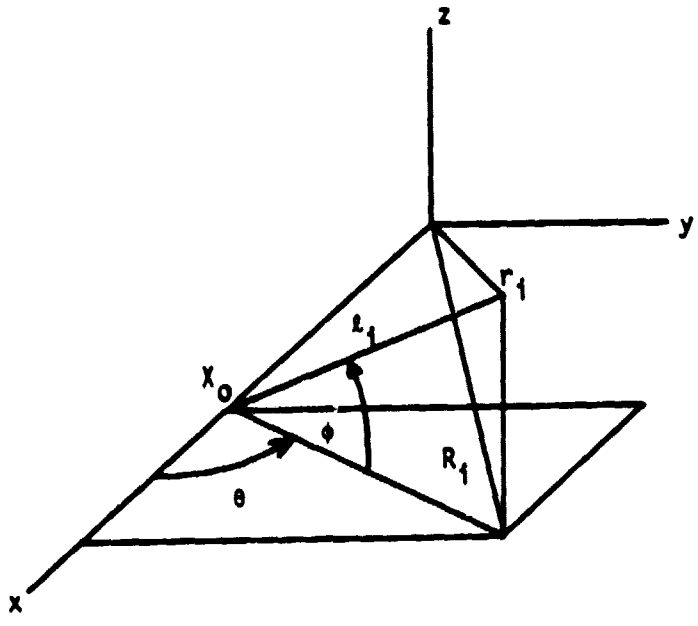

Figure C1

In Figure C1, the Shuttle is located at a distance X_o from the center of the earth along the x-axis. The masses representing the subsatellite and wire elements are located at distances ℓ_i from the Shuttle along a line defined by the angles θ and ϕ. The coordinates of each mass are

$$x_i = X_o + \ell_i \cos\phi\cos\theta \qquad \text{(C1a)}$$

$$y_i = \ell_i \cos\phi\sin\theta \qquad \text{(C1b)}$$

$$z_i = \ell_i \sin\phi \qquad \text{(C1c)}$$

Assuming the system is rotating with constant angular velocity ω about the z-axis, the velocity of each mass is proportional to the distance R_i from the z-axis given by

$$R_i = \sqrt{x_i^2 + y_i^2}$$

The velocity of a mass point is

$$V_i = \omega R_i \tag{C2}$$

The components of the velocity are

$$\dot{x}_i = - V_i \, y_i / R_i$$

$$\dot{y}_i = V_i \, x_i / R_i$$

$$\dot{z}_i = 0 \tag{C3}$$

In order for the system to be in equilibrium in circular orbit, the angular velocity ω must be such that there is no radial acceleration of the system. One condition of equilibrium is that the sum of the gravitational and centrifugal forces on the total system must be zero. In addition, the sum of the tension, centrifugal and gravitational forces on each mass must be zero. The first conditions is given by the equation

$$\sum_i \frac{GMm_i}{r_i^2} = \sum m_i \, r_i \omega^2 \tag{C4}$$

where r_i is the distance of each mass m_i from the center of the earth, and ω is orbital angular velocity. Given the positions and masses of each point, the equilibrium angular velocity can be computed. The point in the system which is at a radial distance ρ defined by the equation

$$\frac{GM}{\rho^2} = \rho \omega^2$$

which can be solved to give

$$\rho = \left(\frac{GM}{\omega^2} \right)^{1/3} \tag{C5}$$

experiences no net radial acceleration. Points above and below ρ experience a net acceleration away from the center.

The condition for equilibrium of the tension forces can be computed using the expression for r given in equation (A27). Setting $\ddot{r} = \ddot{\theta} = \ddot{\phi} = 0.$, and using the exact expression for the gravitational force since the tether length is appreciable, we have

$$F_e/m = GM\ (\rho\cos\theta\cos\phi+r)\ P^{-3} - \dot{\gamma}^2\rho\cos\theta\cos\phi - r\dot{\gamma}^2\cos^2\phi \qquad \text{(C6a)}$$

where

$$P = \sqrt{\rho^2 + 2\rho r\cos\theta\cos\phi + r^2} \qquad \text{(C6b)}$$

and r is the distance from the center of the system.

Using equation (C6), the force on each mass in the Skyhook system can be computed. The tension in each wire segment is equal and opposite to the sum of the forces on all masses which the segment supports. Starting at the end of the system, one can successively compute the tension in each wire segment. Once this tension is known, the natural length ℓ_0 of the wire segment can be computed from the equation

$$\ell_0 = \Delta r\ /\ (1 + \frac{T}{EA}) \qquad \text{(C7)}$$

where Δr is the distance between the masses, E is the elastic modulus, and A the cross sectional area of the wire. Since the mass of each wire segment depends on the natural length which is a function of the tension, the solution for the equilibrium must be iterated to obtain a precise equilibrium configuration.